İSTANBUL UNIVERSITY CERRAHPAŞA

ORIGINAL ARTICLE
Electrica 2024; 24(2): 284-303

Continuous–Discrete Student Psychology-Based Optimization Algorithm for Optimal Planning of Distributed Generators and Distribution Static Compensators in Power Distribution Network

Subrat Kumar Dash[1], Sivkumar Mishra[2]

[1]Department of Electrical Engineering, Government College of Engineering Kalahandi, Bhawanipatna, Odisha, India
[2]Department of Electrical Engineering, Biju Patnaik University of Technology, Odisha, Rourkela, India

Cite this article as: S. Kumar Dash and S. Mishra, "Continuous–discrete student psychology based optimization algorithm for optimal planning of distributed generators and distribution static compensators in power distribution network," *Electrica*, 24(2), 284-303, 2024.

ABSTRACT

In this study, a novel method called the Continuous–Discrete Student Psychology-Based Optimization (CD-SPBO) is introduced. The technique is designed to address the simultaneous allocation of renewable distributed generators (DGs) and distribution static compensators (D-STATCOMs). A novel multi-objective function is formed by combining indices concerning the active power loss, voltage profile, voltage stability and cost consisting of investment, penalty for violation of environmental limits, and energy loss, which are combined through analytic hierarchical process. The CD-SPBO algorithm is used for solving the multi-objective allocation problem for non-dispatchable solar PV-DGs, dispatchable biomass DGs, D-STATCOMs, and their combinations. The superiority of the CD-SPBO algorithm was both numerically and statistically established by comparing its results with other state of the art methods such as Gorilla Troop Optimizer, Artificial Humming Bird Optimizer, and Harris Hawk Optimizer for simultaneous allocation of one, two, and three pairs of DGs and D-STATCOMs on 33-bus and 118-bus test systems. Further, the simulation findings involving seven distinct planning scenarios for the allocation of DGs and D-STATCOMs supported the CD-SPBO algorithm's effective execution for simultaneous optimal allocation of dispatchable DGs, non-dispatchable DGs, and D-STATCOMS. The suitability of different planning scenarios for improving the overall performance of the distribution system are analyzed in detail. The research insights may prove beneficial for network planners in determining the best combination of devices to meet their needs.

***Index Terms*—**Discrete–student psychology-based optimization algorithm, distributed generators, distribution static compensators (D-STATCOMs), power distribution network

Corresponding author:
Sivkumar Mishra

E-mail:
sivmishra@gmail.com

Received: August 20, 2023

Revision Requested: October 4, 2023

Last Revision Received: December 2, 2023

Accepted: December 12, 2023

Publication Date: April 8, 2024

DOI: 10.5152/electrica.2024.23115

I. INTRODUCTION

Distribution utilities (DUs) are currently confronted with the challenge of meeting soaring energy demand arising from the installation of huge industrial loads and many battery charging loads for adopting e-mobility. Therefore, efficient and economic grid management without sacrificing the quality and security of power supply to end users is a major concern for the DUs. With the allocation of active devices like distributed generators (DGs) or distribution flexible transmission (D-FACTS) devices, the distribution system is evolving to be an active power distribution network (APDN). Distributed generators are small-scale power generating units, and distribution static compensators (D-STATCOM) are the D-FACTS devices tailor-made for the distribution level, that can act as the sources of alternate active and reactive power sources. Distributed generators may be powered by solar, wind, tidal, biomass, and other sources. Among these renewable energy technologies, solar energy is the most popular and widely used due to its wide range of applications, including solar pumps, kitchen applications, Electric Vehicle charging stations, and lighting [1], and its ability to meet demand in remote and grid-connected locations [2]. However, power output from the renewable DG is highly susceptible to meteorological conditions. In this regard, biomass-based DGs (BM-DG) are being preferred as they can be dispatchable, have low investment cost, and are portable [3]. Distribution static compensators offers better operational flexibility in terms of continually variable reactive power support, reduced power quality concerns, extended lifespan, but is highly sophisticated and costlier. Distributed generators, on the other hand, offer numerous benefits to the DUs, including reduced real power loss, improved voltage profile, increased voltage stability margin, and reduced transmission burden. Therefore, it is

essential to determine the optimal assignment of these devices so as to provide the necessary technical benefits to the DUs at an affordable investment cost [4].

Several studies have been carried out to select the optimal capacity and position of these active devices individually as well as concurrently to improve the performance of the APDN [1,5]. An equilibrium optimization algorithm-based BM-DG allocation is presented in [6] considering four different loading scenarios with a goal to maximize DUs' benefit in terms of active power loss (APL) reduction and curbing pollutant gas emission. An artificial hummingbird optimization (AHO) is suggested in [7] to mitigate the issues of APL and voltage deviation (VD) by optimally placing BM-DGs. A gravitational search algorithm with improvisation is applied to optimally allocate thin film monocrystalline PV-DGs with the objective of reducing various costs [8]. In another approach, APL reduction is achieved by optimally allocating PV-DGs using a new student psychology-based optimization (SPBO) algorithm in [9]. The allocation of renewable DGs such as PV-DGs and wind turbine DGs is discussed in [10] considering the uncertainty in the DG power generation and variations in load demand using AHO. The authors in [11] proposed an improved bacterial foraging algorithm to improve the performance of the DN by optimally allocating D-STATCOMs. The simultaneous sizing of DGs and D-STATCOMs using different metaheuristic approaches such as modified flower pollination algorithm [12], cuckoo search algorithm [13], whale optimization algorithm [14], and a combination of lightning search and simplex methods [15] are proposed where the potential bus locations for DG and D-STATCOMs are first selected using sensitivity-based approaches. Recently, researchers have proposed new metaheuristic methods, both with and without improvisations, to effectively allocate exclusive DGs [16-19], exclusive D-STATCOMs [20, 21], simultaneous DGs and shunt capacitors (SCs) [22-24], simultaneous DGs and D-STATCOMs [25], as well as combinations of DGs, SCs, static var compensators, and D-STATCOMs to enhance the performance of the DN.

The simultaneous location and sizing of both DGs and D-STATCOMs (optimal allocation DGs and D-STATCOMs (OADD)), using a multiobjective formulation, presents a challenging engineering optimization problem that can be efficiently addressed using metaheuristic methodologies. While metaheuristic techniques possess flexibility and adaptability, they frequently necessitate the adjustment of specific control parameters. The improper parameter settings resulted in being trapped in local optima and a reduced pace of convergence. On the other hand, the SPBO algorithm [26], which is a newly introduced metaheuristic approach, has the ability to efficiently find the best possible solutions at a faster rate without the need for any control parameters, except for the initial population size and the maximum number of function evaluations [27]. Therefore, the authors of this study utilized the SPBO method with a continuous discrete formulation to tackle the issue of allocating simultaneous DGs and D-STATCOMs.

Table I presents a summary of newly proposed approaches for optimal planning of DN that involve the allocation of DGs and D-STATCOMs. The studies [6, 9, 16, 19, 20, 28] defined the allocation problem as a single objective, with a focus on either technical performance [9,16] or economic factors [6, 19, 20, 28]. The allocation problems are also portrayed as a multiobjective formulation, where many technical elements are combined using predetermined weights. It is noteworthy that in the majority of multiobjective formulations, with the exception of [18], many objectives are merged using predetermined weights, which are frequently chosen based on intuition. Since weights have a significant impact on achieving the best possible outcomes, they must be set carefully. The literature analysis also indicates that the placement of DGs or D-STATCOMs is frequently determined in advance utilizing sensitivity techniques, which may not result in the most effective option. The insufficient treatment of both continuous and discrete formulations in addressing continuous decision variables (device capacity) and discrete decision variables (device placement) is also evident from the literature review. Hence, in light of the above discussion the major contributions of the work are outlined below.

(1) The successful implementation of the CD-SPBO algorithm for solving the simultaneous multiobjective optimal allocation of PV DGs, BM DGs, and D-STATCOMs.
(2) The superiority of the CD-SPBO algorithm both numerically and statistically is established by comparing its results with other state-of-the-art methods such as gorilla troop optimizer, AHO and Harris hawk optimizer for the simultaneous allocation of one, two, and three pairs of DGs and D-STATCOMs on a 33-bus and 118-bus test systems.
(3) The multiobjective formulation consists of index of active power loss, the index of overall VD (OVD), the index of minimum voltage stability value, and the index of system annual cost with analytic hierarchical process (AHP)-based optimized weights.
(4) The selection of the suitable combination of PV DGs, BM DGs with D-STATCOMs considering the above proposed indices, neglecting the load variations, is analyzed first.
(5) Finally, the performance of the APDN due to load volatility is assessed in the presence of optimally allocated PV DGs and BM DGs with D-STATCOMs.

II. PROBLEM FORMULATION

Fig. 1 shows a part of an APDN with DGs and D-STATCOM connected to different buses.

A. Active Power Loss Index

The reduction in APL results in financial savings for the utilities, as well as it can improve the reliability of the system. From Fig. 1, APL of the APDN can be computed using (1)

$$P_{loss} = \sum_{j=1}^{nbus} \left| I_m(j) \right|^2 \times R_m(j) \quad (1)$$

where I_m and R_m are the feeder current and resistance, respectively, and *nbus* is the total number of buses of the APDN. The APL index (f_{APL}) is formulated as the ratio of the APL of the APDN with devices (P_{loss}^{device}) to the APL of APDN (P_{loss}^{base}) in the base case.

$$f_{APL} = \frac{P_{loss}^{device}}{P_{loss}^{base}} \quad (2)$$

B. Overall Bus Voltage Deviation Index

Voltage fluctuations are a common phenomenon for long radial feeders and intermittent power injection by renewable DGs. The voltage fluctuates in the distribution buses. For sensitive loads, it is essential to control the voltage of the APDN within regulatory limits. Hence, the OVD of the APDN is calculated using (3).

TABLE I. SUMMARY OF RECENTLY PROPOSED METHODS FOR OPTIMAL PLANNING OF THE DISTRIBUTION NETWORK

			Objectives							
Ref.	**Year**	**Methods**	**RPL**	**VD**	**VSI**	**Cost**	**AHP**	**CD**	**Devices**	**Salient Features**
[7]	2021	EA	x	x	x	√	x	x	Biomass DGs	Optimal allocation of varying numbers of biomass DGs is achieved using EA to maximize the utility benefit and reduce the capital cost of DGs
[10]	2021	SPBO	√	x	x	x	x	x	PV DGs	SPBO algorithm is implemented to solve allocation of PV DGs aiming to minimize RPL.
[17]	2022	IWHO	√	x	x	x	x	x	DGs	IWHO is considered for optimally integrating DGs to improve system reliability. IWHO shows improved balance between exploration and exploitation phase which is essential for solving complex optimization problem
[18]	2022	MOPSO	√	√	√	x	x	x	DGs	Proposed MOPSO integrated with MATPOWER to optimally assign DGs for improvement of various technical performance of the distribution grid.
[19]	2023	mFBI	√	√	√	√	√	x	PV DG and WT DG	mFBI is proposed to decide the optimal allocation of DGs with a goal of improving both technical and economic factors. AHP is introduced to tackle the multicriteria decision making.
[20]	2023	ISSO	x	x	x	√	x	x	PV DG and WT DG	Cost towards power loss and reliability is optimized using ISSO for deciding the optimal allocation of renewable DGs along with network reconfiguration.
[12]	2022	IBFA	√	√	√	x	x	x	D-STATCOM	The performance of the practical Quha feeder is improved by optimally assigning D-STATCOM using IBFA. The results obtained by IBFA are compared against BFA.
[21]	2022	CD-CSA	x	x	x	√	x	√	D-STATCOM	Optimal size and location of the D-STATCOMs are determined by a continuous discrete codification integrated with the sine cosine algorithm with an objective to reduce annual operative cost.
[22]	2023	SMICM	x	x	x	√	x	x	D-STATCOM	Annual installation and operating cost of the 33-bus, 69- bus, and 85-bus test systems are minimized by optimally assigning grid connected D-STATCOMs.
[13]	2018	mFP	√	√	√	x	x	x	PV DGs, NR and D-STATCOMs	The optimal sizing of DGs and D-STATCOMs are accomplished by mFP algorithm at strategic locations determined using voltage stability index.
[14]	2018	CSA	√	√	x	x	x	x	DGs and D-STATCOMs	Location of DGs and D-STATCOMs is first determined using sensitivity approaches followed by optimal sizing using CSA.
[15]	2020	WOA	√	x	x	√	x	x	DGs and D-STATCOMs	Simultaneous optimal capacities of DGs and D-STATCOMs are computed to minimize loss and operating cost. Loss sensitivity factor is used to locate the placements of devices.
[23]	2022	BES	√	√	√	x	x	x	DGs, SC, D-STATCOM, SVC	The performance of the 33-bus and 118- bus systems is improved through optimal allocation of DGs and different shunt reactive compensators like D-STATCOM, SVC, and shunt capacitor. BES is implemented to decide the location and sizes of the devices.
[24]	2023	IGJO	√	√	√	x	x	x	Type-I and Type-III DGs, SC	IGJO is proposed to optimally allocate DGs and capacitors at predetermined locations as obtained by a sensitivity approach to enhance the performance of the distribution system.
[25]	2023	LTCO	√	√	√	x	x	x	DGs and SC	Sensitivity indices are used to predetermine the potential buses for DG and SC injections. LTCO is proposed for the distribution network planning in presence of DGs and SCs considering different voltage dependent load models.
[26]	2023	MGSA-EE	√	√	x	x	x	x	DGs and SC	Optimal allocation of DGs and SCs is solved using MGSA-EE to minimize power loss and voltage deviation.
[27]	2023	DMO	√	√	x	x	x	x	DGs and D-STATCOMs	DMO is proposed to optimally allocate DGs and D-STATCOMs to enhance the technical performance of the distribution network where the locations of DG and SC are predetermined using a sensitivity approach.

AHP, analytic hierarchical process; BES, bald eagle search; CD-CSA, continuous–discrete sine cosine algorithm; CSA, cuckoo search algorithm; DMO, dwarf mongoose optimization; D-STATCOM, distribution static compensators; EA, equilibrium algorithm; IBFA, improved bacterial foraging search algorithm; IGJO, improved golden jackal optimization; ISSO improved salp swarm optimization; IWHO, improved wild horse optimization; LTCO, Lichtenberg and thermal exchange optimization; MGSA-EE, modified gravitational search with expert experience; mFBI, modified forensic based investigation; NR, network reconfiguration; RPL, real power loss; SC, shunt capacitor; SMICM, stochastic mixed-integer convex model; SPBO, student psychology-based optimization; SVC, static voltage compensator; VSI, voltage stability index.

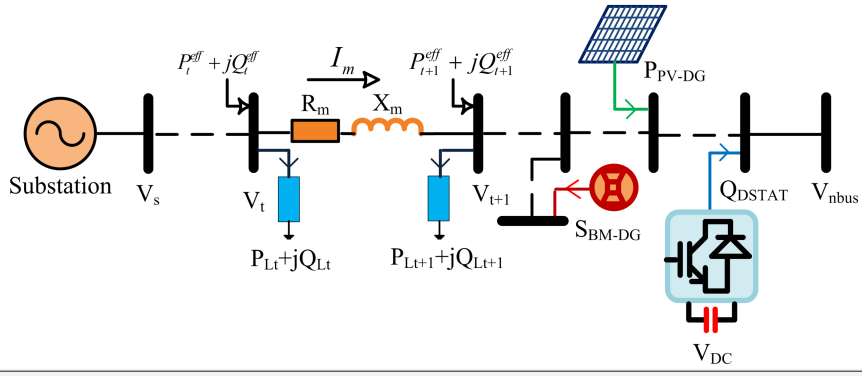

Fig. 1. A part of APDN with DGs and D-STATCOM.

$$OVD = \sum_{t=1}^{nbus} (V_t - V_s)^2 \tag{3}$$

where V_t and V_s are the voltage magnitudes of t^{th} bus and substation bus, respectively. To assess the impact of the allocation of the devices on the OVD of the APDN, the OVD index (f_{OVD}) is defined in (4).

$$f_{OVD} = \frac{OVD^{device}}{OVD^{base}} \tag{4}$$

where OVD^{device} and OVD^{base} are the VD of the APDN with and without installation of devices respectively.

C. Critical Voltage Stability Index

Large reactive power demands caused by the addition of nonlinear loads can jeopardize the stability of the APDN. The voltage stability index (VSI) is used to assess the stability of the DN, which is computed using Equation (5).

$$VSI(t+1) = |V_t|^4 - 4\left[P_{t+1}^{eff} \times X_m - Q_{t+1}^{eff} \times R_m\right]^2 - 4\left[P_{t+1}^{eff} \times R_m + Q_{t+1}^{eff} \times X_m\right]|V_t|^2 \tag{5}$$

where X_m is the reactance of the feeder; P_{t+1}^{eff} and Q_{t+1}^{eff} are the effective real and reactive power injection at bus (t+1) as shown in Fig. 1.

The bus having minimum VSI is designated as the critical bus, and the corresponding VSI value is labeled as critical VSI (CVSI) which is computed using (6).

$$CVSI = \min(VSI(t+1))\ t = 1,2,3\cdots nbus - 1 \tag{6}$$

The factor of critical VSI (f_{CVSI}) is formulated in (7) to assess the impact of device allocations on the stability of the APDN.

$$f_{CVSI} = \frac{1/CVSI^{devics}}{1/CVSI^{base}} \tag{7}$$

where $CVSI^{devics}$ and $CVSI^{base}$ are respectively the CVSI with and without allocation of devices.

D. System Annual Cost index

The DUs purchase power from the upstream grid and generate revenue by selling it directly to the consumer. Assuming the power purchased by the DUs is generated by burning of fossil fuels, it incurs additional penalty cost towards emission of greenhouse gases. Hence, when no devices are put in the APDN, the annual cost of DU (AC^{base}) includes the annual cost of power purchased by DU (PC_{sub}^{base}) and emission penalty cost (EC_{sub}^{base}) for resulting emissions as demonstrated in (8, 9,10).

$$AC^{base} = PC_{sub}^{base} + EC_{sub}^{base} \tag{8}$$

$$PC_{sub}^{base} = k_{sub}^{real} \times P_{sub}^{base} \times 8760 + k_{sub}^{reac} \times Q_{sub}^{base} \tag{9}$$

$$EC_{sub}^{base} = E_{sub} \times k_{em}^{sub} \times P_{sub}^{base} \times 8760 \tag{10}$$

where k_{sub}^{real} and k_{sub}^{reac} are the cost coefficients in USD/kW and USD/kVAr, respectively; P_{sub}^{base} and Q_{sub}^{base} are the substation real and reactive power; E_{sub} is the emission caused by the substation; and k_{sub}^{em} is the emission cost coefficient of the substation. The factor 8760 accounts for the total number of hours per year.

However, when new devices (DGs or D-STATCOMs) are added, the DU must share the capital cost as well as the operation and maintenance costs of the equipment (C^{device}), in addition to the power purchase cost (PC^{device}) and emission cost (EC^{device}) for power drawl from the grid as outlined in (11, 12, 13, 14).

$$AC^{device} = C^{device} + PC^{device} + EC^{device} \tag{11}$$

$$PC^{device} = k_{sub}^{real} \times P_{sub}^{device} \times 8760 + k_{sub}^{reac} \times Q_{sub}^{device} \tag{12}$$

$$EC^{device} = E_{sub}^{em} \times k^{em} \times P_{sub}^{device} \times 8760 + E_{DG}^{em} \times k^{em} \times P_{sub}^{device} \times 8760 \tag{13}$$

$$C^{device} = \frac{IC^{device}}{LS^{device}} + OM^{device} \tag{14}$$

where P_{sub}^{device} and Q_{sub}^{device} are the substation real and reactive power in presence of DGs and D-STATCOMs; k_{dg}^{em} is the emission cost coefficient of the substation; E_{DG} is the emission caused by biomass DG; IC^{device}, $OM^{device}$and LS^{device} are the installation cost, operation and maintenance cost, and life span of the devices respectively.

Undoubtedly, the inclusion of the devices reduces the cost towards energy purchase and emissions, resulting in a net annual cost reduction as compared to the base case which can be assessed by the system annual cost index (f_{SAC}) as defined in (15).

$$f_{SAC} = \frac{AC^{device}}{AC^{base}} \tag{15}$$

E. Formulation of Multi-Objective Function

To determine the optimal allocation of the devices, the multi-objective function (MOF) consisting of the above techno-economic indices is formulated as expressed in (16).

$$f = \min(w_1 f_{APL} + w_2 f_{ovd} + w_3 f_{cvsi} + w_4 f_{SAC}) \tag{16}$$

The MOF combines the four indices using weighting factors (w_1, w_2, w_3, and w_4) which play a decisive role in the final optimal solution. In this work, these weighting factors are judiciously selected using the AHP [29].

F. Constraints

The following constraints were considered while optimizing the MOF:

1) Power Balance Constraint

The net real and reactive power available at the substation, including power import from the upstream grid and that supplied by DGs and D-STATCOMs, must be balanced by the net real and reactive demand of the APDN, including losses as expressed in (17–18).

$$P_{slack} + \sum_{j=1}^{ndg} P_{DG,j} = \sum_{t=1}^{nbus} P_{l,t} + P_{loss} \tag{17}$$

$$Q_{slack} + \sum_{j=1}^{ndstat} Q_{DSTATCOM,j} = \sum_{t=1}^{nbus} Q_{l,t} + Q_{loss} \tag{18}$$

where P_{DG} and $Q_{DSTATCOM}$ are the sizes of DG and D-STATCOM, respectively; *ndg* and *ndstat* are the number of DGs and D-STATCOMs to be connected to the APDN, respectively.

2) Bus Voltage Constraint

The bus voltage is regulated using the following constraint to ensure the voltage at all buses stays within the regulatory limits of 0.95 p.u. to 1.05 p.u.

$$0.95 < V_t < 1.05 \tag{19}$$

3) Device Capacity Constraints

The total sizes of DGs and D-STATCOMs must be lower than the total real and reactive power demand of the APDN, which are ensured by implementing the following capacity constraints.

$$\sum_{j=1}^{ndstat} Q_{DSTATCOM,j} \le \sum_{t=1}^{nbus} Q_{l,t} \tag{20}$$

$$\sum_{j=1}^{ndg} P_{DG,j} \le \sum_{t=1}^{nbus} P_{l,t} \tag{21}$$

III. OPTIMIZATION ALGORITHM

In this work, a new SPBO algorithm with continuous discrete codification is proposed to solve the simultaneous allocation of DGs and D-STATCOMs. In SPBOA, the psychology of students to retain or become the top scorer of the class resembles the optimization process. Similar to other metaheuristic approaches, SPBOA also begins with an initial population (termed as class) which consists of a set of student performances (search agent) in different subjects (decision variables). The initial population is then iteratively evolved, governed by the performance improvement of students belonging to aforementioned groups, in order to reach the global optima. Since the locations of devices are discrete variables, a Euclidian norm-based codification is adopted to discretize the location variables in each iteration before the fitness evaluation. The detailed steps for implementation of the proposed continuous–discrete student psychology-based optimization algorithm (CD-SPBOA) for solving simultaneous OADD are described below.

A. Generation of Initial Population

The initial population is constructed using (22).

$$P = \begin{bmatrix} p_{11} & p_{12} & \cdots & p_{1D} \\ p_{21} & p_{22} & \cdots & p_{2D} \\ \vdots & \vdots & \ddots & \vdots \\ p_{N1} & p_{N2} & \cdots & p_{ND} \end{bmatrix} \tag{22}$$

where D and N denote the number of decision variables and population size of the optimization problem, respectively. In this article, each row of the population, P, contains the sizes ($size_{device,1}$ … $size_{device,n}$) and locations ($loc_{device,1}$ … $loc_{device,n}$) of the devices as per (23).

$$P_i = \left[size_{device,1}, ..., size_{device,n}, loc_{device,1}, ..., loc_{device,n} \right] \tag{23}$$

The sizes of the devices are modeled as continuous variables, whereas the locations are modeled as discrete variables. Therefore, each component of the initial population is generated randomly to distribute over the entire search space of the optimization problem using (24–25).

$$size_{device,j} = size_{\min} + rand(size_{\max} - size_{\min}) \tag{24}$$

$$loc_{device,j} = loc_{\min} + rand(loc_{\max} - loc_{\min}) \tag{25}$$

where $size_{max}$ and $size_{min}$ are the maximum and minimum capacities of the devices and loc_{max} and loc_{min} are the maximum and minimum allowable positions of the devices respectively. To discretize the locations, the Euclidian norm-based, nearest vortex approach is employed. The discrete variables are usually expressed as sets of ordered pairs, which constitutes a hypercube as expressed in (26).

$$loc^{H}_{device,j} = \left\{ \left(loc^{L}_{device,j}, loc^{H}_{device,j} \right) \middle| loc_{device,j} \in ¢, j \in 1,2,...,n \right\} \tag{26}$$

Where $loc^{H}_{device,j}$ and $loc^{L}_{device,j}$ are respectively the upper and the lower range of the j^{th} variable in the hypercube $loc^{H}_{device,j}$. The floor and ceiling functions as described in (2728) are then used to describe the upper and the lower limits in the hypercube.

$$loc^{H}_{device,j} = \max\left\{ loc_j \in ¢^{+} \middle| loc_j \le loc_{device,j} \right\} \tag{27}$$

$$loc^{L}_{device,j} = \min\left\{ loc_j \in ¢^{+} \middle| loc_j \ge loc_{device,j} \right\} \tag{28}$$

where $¢^{+}$ is the set of integers. Now, the discrete variable is computed using (34).

$$loc^{dis}_{device,j} = \begin{cases} loc^{H}_{device,j}, if \left| loc_{device,j} - loc^{L}_{device,j} \right| > \left| loc_{device,j} - loc^{H}_{device,j} \right| \\ loc^{L}_{device,j}, if \left| loc_{device,j} - loc^{L}_{device,j} \right| \le \left| loc_{device,j} - loc^{H}_{device,j} \right| \end{cases} \quad (29)$$

B. Evolution of the Population

In recognition of the various ways in which students may enhance their performance, the entire class is randomly divided into four groups, taking into account the distinct psychological characteristics of each student. The first group consists of the top-performing student (typically the student with the highest score in the evaluation). The second group comprises students who excel in specific subjects. The third group consists of students who put in average effort to improve their performance. The fourth group consists of students who have no structured approach to enhance their performance and are below average. The performance improvement of students from the aforementioned groups is described below.

1) Performance improvement of the best student

A best student secures the highest total mark by performing better than any student in the class as demonstrated in (30)

$$p^{k+1}_{best,j} = p^{k}_{best,j} + (-1)^{\alpha} \times rand \times \left(p^{k}_{best,j} - p^{k}_{rj} \right) \quad (30)$$

For the j[th] subject, the marks secured by the best student and any other student of the class are denoted as $p^{k}_{best,j}$ and p^{k}_{rj} respectively. *rand* is a random number in the range [0,1]. *a* can be 1 or 2.

2) Performance improvement of good students

Few good students will be influenced by the best student and therefore try to perform similarly to the best student as modeled in (31). Others, on the other hand, may try to perform better than the average students of the class and at the same time try to chase the performance of the best student as modeled in (32).

$$p^{k+1}_{i,j} = p^{k}_{best,j} + rand \times \left(p^{k}_{best,j} - p^{k}_{i,j} \right) \quad (31)$$

$$p^{k+1}_{i,j} = p^{k}_{i,j} + \left| rand \times \left(p^{k}_{best,j} - p^{k}_{i,j} \right) \right| + \left| rand \times \left(p^{k}_{i,j} - p^{k}_{avg} \right) \right| \quad (32)$$

where $p^{k}_{i,j}$ corresponds to the marks obtained by the i[th] student in the j[th] subject and p^{k}_{avg} denotes the average marks of the class for the j[th] subject

3) Performance improvement of average students

Since efforts made by students are contingent upon their interest in the respective subjects, they offer an average try to the subject that has little interest for them. While they may put additional effort into other subjects to boost their overall grades. So, an average student may improve his performance as per equation (33)

$$p^{k+1}_{i,j} = p^{k}_{i,j} + \left| rand \times \left(p^{k}_{avg} - p^{k}_{i,j} \right) \right| \quad (33)$$

4) Performance improvement of below average students

Below average students. attempt to enliven their overall score arbitrarily. Their performance improvement can be signified as:

$$p^{k+1}_{i,j} = p^{\min}_{j} + \left[rand \times \left(p^{\max}_{j} - p^{\min}_{j} \right) \right] \quad (34)$$

where $p^{\max}_{j}$ and $p^{\min}_{j}$ corresponds to the legitimate range of maximum and minimum score against the subject under consideration.

IV. METHODOLOGY

In this work, the CD-SPBOA is proposed to determine the simultaneous OADD considering a MOF to improve the performance of the APDN. To select the economically viable appropriate combinations of devices for facilitating the performance improvement of the APDN, seven different planning schemes (PS) excluding the base case are generated.

PS-I: APDN with three optimally allocated D-STATCOMs

PS-II: APDN with three optimally allocated PV-DGs

PS-III: APDN with three optimally allocated BM-DGs

PS-IV: APDN with simultaneous optimally allocated three D-STATCOMs and three PV-DGs

PS-V: APDN with simultaneous optimally allocated three D-STATCOMs and three BM-DGs

PS-VI: APDN with simultaneous optimally allocated three D-STATCOMs, two PV-DGs, and one BM-DG

PS-VII: APDN with simultaneous optimally allocated three D-STATCOMs, one PV-DG, and two BM-DGs.

The detailed flowchart for the implementation of CD-SPBOA for obtaining the optimal PS considering allocation of different combinations of D-STATCOMs, PV DGs, and BM DGs is presented in Fig. 2.

V. RESULTS AND DISCUSSION

To validate the proposed methodology for simultaneous allocation of DGs and D-STATCOMs, a standard 33-bus APDN [30] and a larger 118-bus test system have been considered. When no devices are installed, the 33-bus system has a real and reactive power loss of 210 kW and 143 kVAr, respectively, and the 18th bus registers a minimum bus voltage of 0.9038 p.u., which is far below the regulatory limit of 0.95 p.u. Similarly, the real and reactive power losses of the 118-bus system are 12981 kW and 978.7 kVAr, respectively, and the minimum bus voltage is 0.8688 p.u. for the uncompensated system. The maximum capacity of DGs and D-STATCOMs considered in the analysis is 2000 kW and 2000 kVAr for the 33-bus system and 4000 kW and 3000 kVAr for the 118-bus test system respectively. The best results from 30 independent trial runs of the CD-SPBO algorithm have been reported. The population size and the maximum number of iterations of CD-SPBOA were set at 50 and 100, respectively, for all the studied planning scenarios for both test systems. A forward–backward sweep load flow [31] is utilized to capture the snapshot of the APDN with and without allocation of devices for calculation of MOF. All the simulation work is carried out using MATLAB software. The technical, economic, and environmental parameters of the substation, DGs, and D-STATCOMs are described in Table II. Results of interest are boldfaced in respective tables.

A. Validation of CD-SPBOA for Solving OADD

Table III compares the results obtained by CD-SPBO and other competing algorithms in addressing OADD to minimize real power loss on a 33-bus test system taking into account different combinations of the devices. From Table III, it may be noted that the real power loss (RPL) reported by CD-SPBOA is the minimum for simultaneous

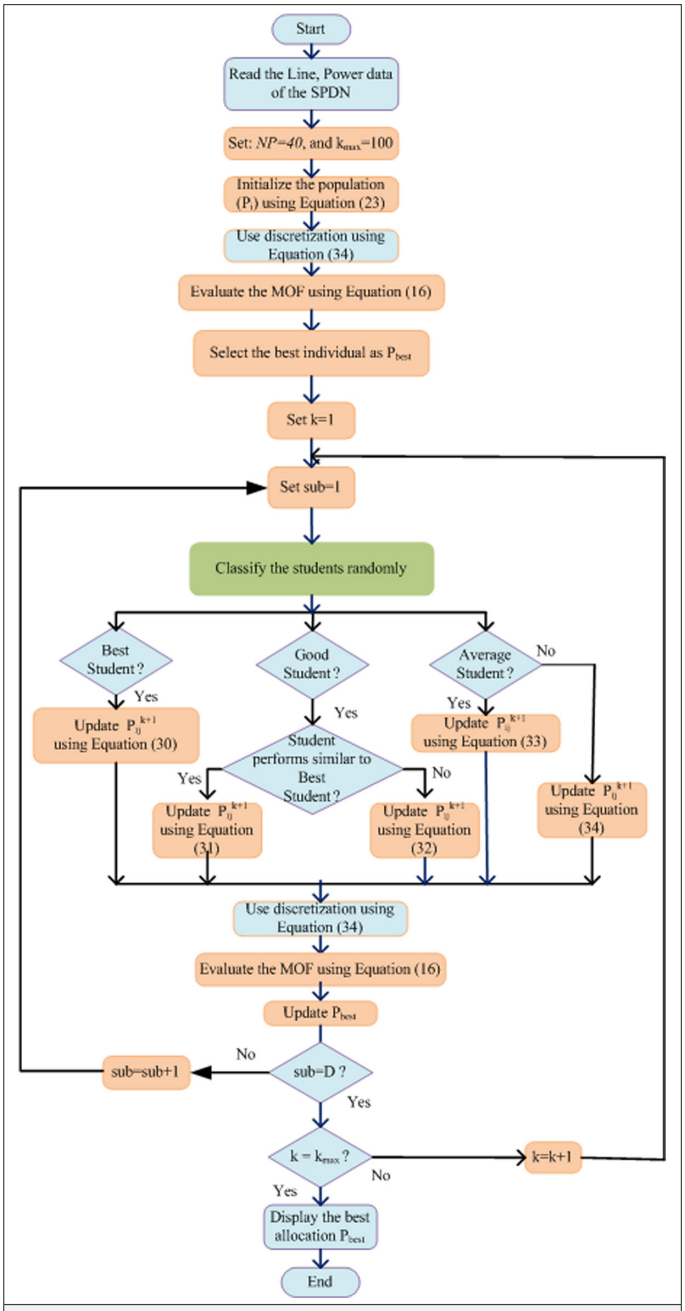

Fig. 2. Implementation of proposed CD-SPBOA for optimal SPDN planning. MOF, multi-objective function; SPDN, Smart Power Distribution Network.

allocations of a combination of one and two pairs of the devices. However, for the allocation of three DGs and D-STATCOMs, the RPL obtained by whale optimization and loss sensitive factor [14] is marginally better compared to CD-SPBOA. However, the performance of the CD-SPBOA can be considered superior as it simultaneously optimizes both the location and sizes of the devices in contrast to optimizing only the sizes of the devices at pre-located buses as reported in [12-14, 32, 33]. Similarly, the allocation of different combinations of DGs and D-STATCOMs to minimize RPL in a 118-bus test system is depicted in Table IV. In terms of minimum RPL, the performance of the CD-SPBOA is far superior compared to the recently surfaced

TABLE II. SUBSTATION, DG, AND D-STATCOM PARAMETERS

	Parameter Value			
Parameters	**Substation**	**Photovoltaic Distributed Generator (PV-DG)**	**BM-DG**	**D-STATCOM**
k_{sub}^{real} USD/MWh	78	-	-	-
k_{sub}^{reac} USD/MVAr	5230	-	-	-
k^{em} USD/TonCO_2	10	-	10	-
E_{sub}^{em}, E_{DG}^{em} (TonCO_2/MWh)	0.910	-	0.773	-
IC^{device} (USD/kVA)	-	2000	1.030	50
OM^{device} (USD/kVA)	-	1% of IC	0.085	5% of IC
LS^{device} years	-	30	10	30

BM-DG, Bio-mass-based distributed generator; D-STATCOM, distribution static compensators; PV-DG, Photovoltaic Distributed Generator.

metaheuristic approaches like gorilla troop optimizer (GTO), Harris hawk optimizer (HHO), and AHO.

The convergence characteristics of CD-SPBO against GTO, HHO, and AHO for solving simultaneous DG and D-STATCOM allocation considering different combinations of the devices are shown in Figs. 3–5 for the 33-bus test systems and in Fig. 6 to Fig. 8 for the 118-bus test systems respectively. From these figures, it may be noted that with an increase in the number of devices as well as for the larger test system, the proposed CD-SPBO outperforms the remaining algorithms in terms of faster convergence and the capability to reach the minimum objective value.

Further, for statistical validation, box plots of the results obtained by CD-SPBO, GTO, HHO, and AHO for solving simultaneous OADD in a 33-bus and 118-bus test systems are presented in Figs. 9–14. It may be seen from these plots that the box plot corresponding to the CD-SPBO is smaller compared to the remaining approaches, which statistically proves the superiority and robustness of the proposed CD-SPBO for solving the simultaneous OADD against the compared approaches.

B. Optimal Planning of APDN using CD-SPBOA

It is evident from the previous section that the proposed CD-SPBOA is both numerically and statistically promising to solve the simultaneous OADD problem. Therefore, in this section, the allocation of non-dispatchable PV-DGs, dispatchable BM-DGs, D-STATCOMs, and their combinations are optimally allocated using the proposed CD-SPBOA for deciding the optimal planning of the APDN with the goal of enhancing the technical performance and minimizing the annual cost of the DUs. Hence, for all the planning scenarios, both the sizes and locations of the devices are simultaneously optimized where the sizes of the devices are treated as continuous variables and the locations of the devices are considered to be discrete. The proposed methodology for optimal APDN planning is also validated considering a 33-bus and a bigger 118-bus test systems. In this work, PV DGs and BM-DGs are considered to operate at unity power factor and combined load power factor respectively. Hence, PV DGs

TABLE III. RESULT COMPARISON OF CD-SPBOA AGAINST OTHER COMPETITIVE APPROACHES FOR SOLVING OADD ON A 33-BUS SYSTEM

Devices	Method	P_{DG}, kW	L_{DG}	Q_{DSTAT}, kVAr	L_{DSTAT}	P_{loss}, kW	Q_{loss}, kVAr	V_{min} p.u.	CVSI p.u.
1 DG + 1 DSTATCOM	GTO	2000	7	1000	30	57.3096	41.7881	0.9549	0.8314
	HHO	1.9950	7	0.9938	30	57.4816	41.8582	0.9548	0.8310
	AHO	1.9992	7	0.9972	30	57.3698	41.8188	0.9549	0.8313
	CD-SPBO	2000	7	1000	30	**57.3096**	**41.7881**	**0.9549**	**0.8314**
	LSF [33]	1000	30	1500	30	86.26	-	0.9503	-
	FP & CS [13]	1323.6	33	1481	31	65.7	-	0.9612	-
2 DGs + 2 DSTATCOMs	GTO	0.8106	14	0.4688	12	29.8556	21.4390	0.9803	0.9236
		1.2460	30	0.8592	30				
	HHO	0.9121	13	0.6615	9	29.5403	20.8882	0.9804	0.9238
		1.0342	30	0.9128	30				
	AHO	1.0857	30	0.5828	9	29.4810	20.7849	0.9799	0.9220
		0.7349	14	0.9925	30				
	CD-SPBO	1.1332	30	1.0000	30	**28.5224**	**20.3363**	**0.9803**	**0.9235**
		0.8414	13	0.4699	12				
3 DGs + 3 DSTATCOMs	GTO	1.2070	24	0.3547	14	15.0594	11.6482	0.9924	0.9697
		1.0153	12	0.9824	30				
		0.7338	31	0.9823	3				
	HHO	0.6249	13	0.5236	5	16.4771	13.5047	0.9815	0.9282
		1.1343	29	0.1244	16				
		1.0334	24	0.9566	30				
	AHO	1.1176	30	0.2684	13	15.1386	12.3360	0.9881	0.9532
		0.9625	25	0.7153	30				
		0.6846	13	0.6137	6				
	CD-SPBO	1.0853	24	0.3714	13	11.6630	**9.6484**	**0.9919**	**0.9660**
		0.7543	14	0.4787	24				
		1.0212	30	1.0000	30				
	CS & LSF [14]	750	14	420	11	12	-	0.9910	0.9584
		1100	24	460	24				
		1000	30	970	30				
	WO & LSF [15]	710	14	380	11	**11.56**	-	0.9913	0.9596
		1040	24	480	24				
		1020	30	980	30				
	MODE [33]	1072	14	521	12	12.95	-	0.9911	-
		742	25	476	25				
		947	30	1018	30				

AHO, artificial hummingbird optimizer; CD-SPBO, continuous–discrete student psychology-based optimization; CS, clonal selection; CSO, cuckoo search optimization; CVSI, critical voltage stability index; D-STATCOM, distribution static compensators; FP, flower pollination; GTO, gorilla troop optimizer; HHO, Harris hawk optimizer; LDG, DG connected bus; LDSTAT, D-STATCOM connected bus; LSF, loss sensitive factor; MODE, multiobjective differential evolution; P_{DG}, real power injected by DG; P_{loss}, real power loss; Q_{DSTAT}, reactive power injected by D-STATCOM; Q_{loss}, reactive power loss; V_{min}, minimum bus voltage; WO, whale optimization. Bold values represent the best values.

TABLE IV. RESULT COMPARISON OF CD-SPBOA AGAINST OTHER COMPETITIVE APPROACHES FOR SOLVING OADD ON THE 118-BUS SYSTEM

Devices	Method	P_{DG}, kW	L_{DG}	Q_{DSTAT}, kVAr	L_{DSTAT}	P_{loss}, kW	Q_{loss}, kVAr	V_{min} p.u.	CVSI p.u.
1 DG + 1 DSTATCOM	GTO	3.0879	71	2.3334	110	872.8667	698.0170	0.9095	0.6842
	HHO	2.9567	71	2.5141	110	871.9511	697.9022	0.9095	0.6842
	AHO	3.0264	71	2.5506	110	872.0580	697.1431	0.9095	0.6842
	CD-SPBO	2.9786	71	2.4973	110	**871.9319**	**697.7693**	**0.9095**	**0.6842**
2 DGs + 2 DSTATCOMs	GTO	2.7134	110	2.3565	50	601.3990	474.0103	0.9447	0.7966
		3.0709	71	1.3471	74				
	HHO	2.5975	110	2.6396	49	578.4101	475.1972	0.9467	0.8032
		3.1466	70	2.1702	111				
	AHO	3.0716	72	1.7258	110	579.4776	477.8930	0.9484	0.8089
		2.5991	110	2.6033	50				
	CD-SPBO	2.9785	71	2.3226	110	**567.1219**	**468.6860**	**0.9501**	**0.8150**
		2.7998	110	2.7266	50				
3 DGs + 3 DSTATCOMs	GTO	3.1176	35	1.4949	110	432.0416	308.6070	0.9537	0.8272
		2.9245	71	2.7987	52				
		2.0664	107	2.0481	70				
	HHO	2.3647	52	1.5492	71	378.4673	286.9929	0.9585	0.8442
		2.1752	110	2.6154	50				
		2.7517	74	2.6387	110				
	AHO	3.7086	109	2.1145	106	421.0834	307.5153	0.9523	0.8225
		1.8710	71	2.8594	50				
		3.1144	48	1.3535	75				
	CD-SPBO	2.9315	71	2.5935	50	**344.3700**	**259.2236**	**0.9600**	**0.8495**
		2.7997	110	1.8310	72				
		2.8744	50	2.3219	110				

AHO, artificial hummingbird optimizer; CD-SPBO, continuous–discrete student psychology-based optimization; CVSI, critical voltage stability index; GTO, gorilla troop optimizer; D-STATCOM, distribution static compensators; HHO, Harris hawk optimizer; LDG, DG connected bus; LDSTAT, D-STATCOM connected bus; P_{DG}, real power injected by DG; P_{loss}, real power loss; Q_{DSTAT}, reactive power injected by D-STATCOM; Q_{loss}, reactive power loss; V_{min}, minimum bus voltage. Bold values represent the best values.

can support active power only whereas BM-DGs can inject reactive power in addition to active power.

1) 33-bus APDN

The results obtained by CD-SPBOA for minimizing the proposed MOF considering different planning scenarios for a 33-bus APDN are presented in Table V. From Table V, it may be noted that the reduction in APL and improvement in voltage profile is better and more or less similar for planning scenarios involving simultaneous allocation of both DGs and D-STATCOMs (PS-IV to PS-VII) owing to the concurrent real and reactive power injection compared to exclusive device allocation. Furthermore, in PS-V, additional reactive power is also supported by BM-DGs in addition to that of D-STATCOMs, leading to maximum APL reduction and enhanced voltage profile compared to the remaining scenarios. However, in terms of overall performance improvement, PS-IV has delivered the best, followed by PS-VI, as indicated by the least MOF values reported in Table V.

The convergence characteristics of CD-SPBOA for minimizing the proposed MOF considering different planning scenarios are depicted in Fig. 15. It shows that CD-SPBOA converges swiftly to the optimal value for all planning scenarios and attains the minimum MOF for PS-IV followed by PS-VI. The voltage profile of the 33-bus APDN corresponding to all planning scenarios is also compared in Fig. 16. It displays that the base case voltage profile of the 33-bus APDN is not acceptable as many of the bus's voltage magnitudes are less than the regulatory limits of 0.95 p.u. However, for planning scenarios PS-III to PS-VII, the voltage profile of the network is significantly improved.

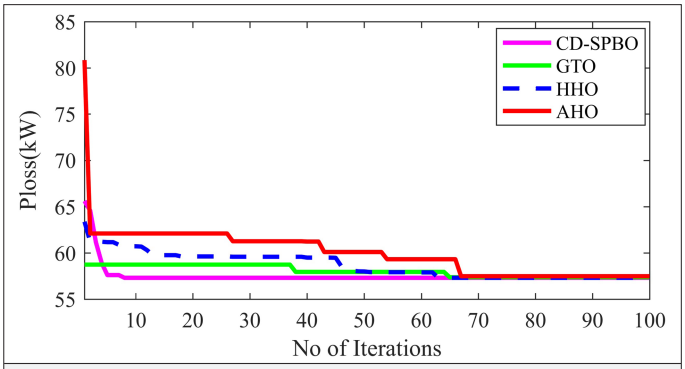

Fig. 3. Comparison of the convergence characteristic for optimal allocation of one DG and one D-STATCOM in a 33-bus system. AHO, artificial hummingbird optimizer; CD-SPBO, continuous–discrete student psychology-based optimization; GTO, gorilla troop optimizer; HHO, Harris hawk optimizer.

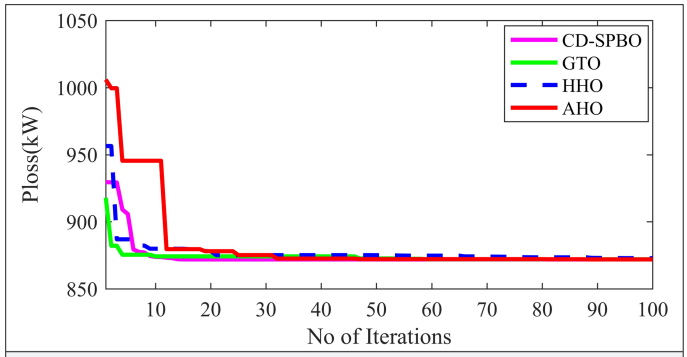

Fig. 6. Comparison of the convergence characteristic for optimal allocation of one DG and one D-STATCOM in a 118-bus system. AHO, artificial hummingbird optimizer; CD-SPBO, continuous–discrete student psychology-based optimization; GTO, gorilla troop optimizer; HHO, Harris hawk optimizer.

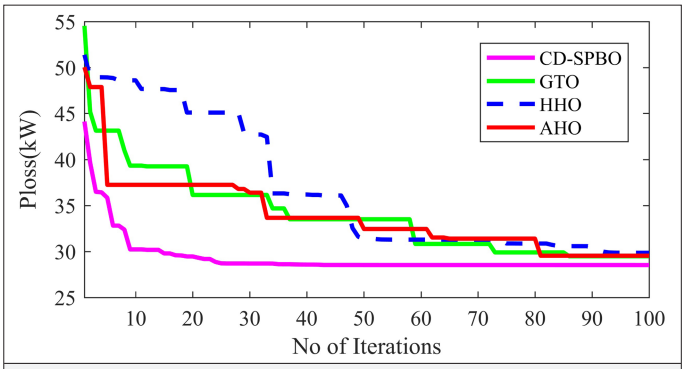

Fig. 4. Comparison of the convergence characteristic for optimal allocation of two DGs and two D-STATCOMs in a 33-bus system. AHO, artificial hummingbird optimizer; CD-SPBO, continuous–discrete student psychology-based optimization; GTO, gorilla troop optimizer; HHO, Harris hawk optimizer.

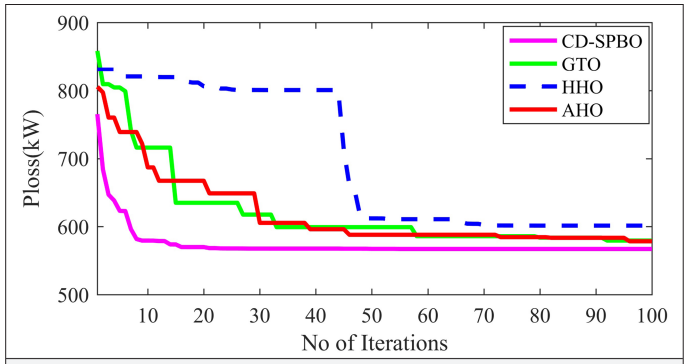

Fig. 7. Comparison of the convergence characteristic for optimal allocation of two DGs and two D-STATCOMs in a 118-bus system. AHO, artificial hummingbird optimizer; CD-SPBO, continuous–discrete student psychology-based optimization; GTO, gorilla troop optimizer; HHO, Harris hawk optimizer.

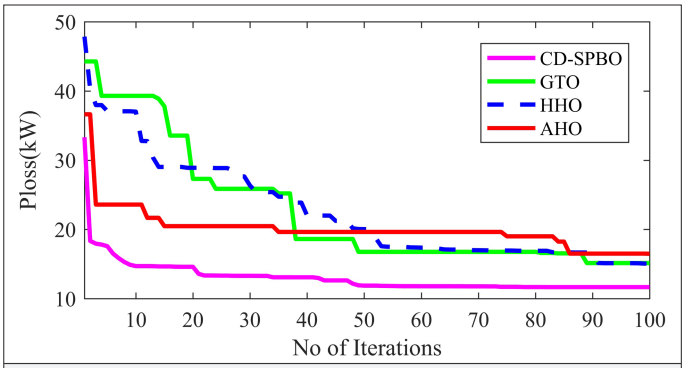

Fig. 5. Comparison of the convergence characteristic for optimal allocation of three DGs and three D-STATCOMs in a 33-bus system. AHO, artificial hummingbird optimizer; CD-SPBO, continuous–discrete student psychology-based optimization; GTO, gorilla troop optimizer; HHO, Harris hawk optimizer.

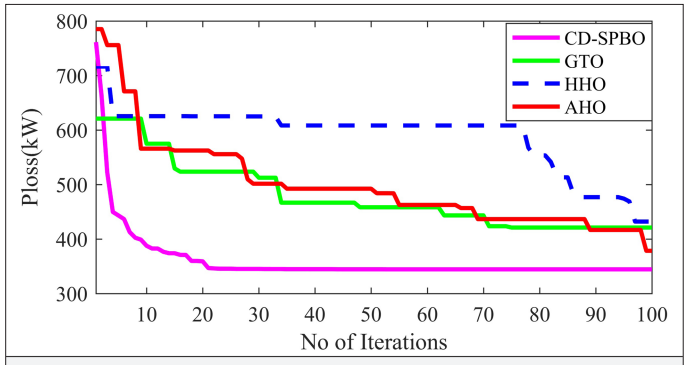

Fig. 8. Comparison of the convergence characteristic for optimal allocation of three DGs and three D-STATCOMs in a 118-bus system. AHO, artificial hummingbird optimizer; CD-SPBO, continuous–discrete student psychology-based optimization; GTO, gorilla troop optimizer; HHO, Harris hawk optimizer.

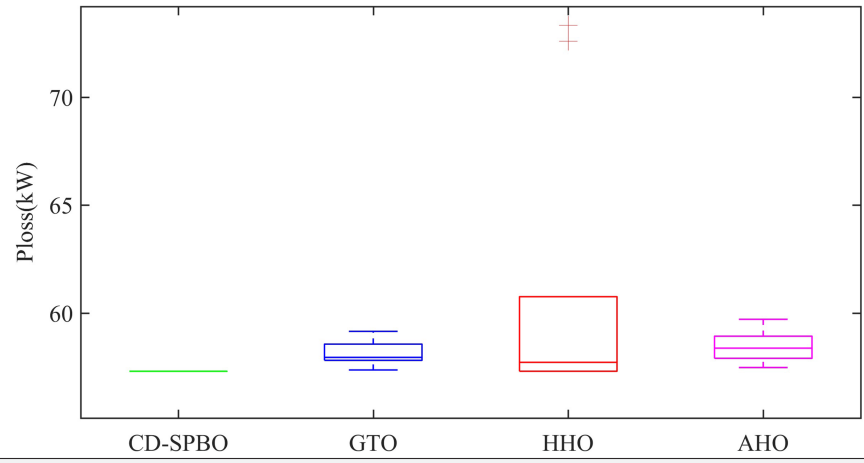

Fig. 9. Box plot for optimal allocation of one DG and one D-STATCOM in a 33-bus system. AHO, artificial hummingbird optimizer; CD-SPBO, continuous–discrete student psychology-based optimization; GTO, gorilla troop optimizer; HHO, Harris hawk optimizer.

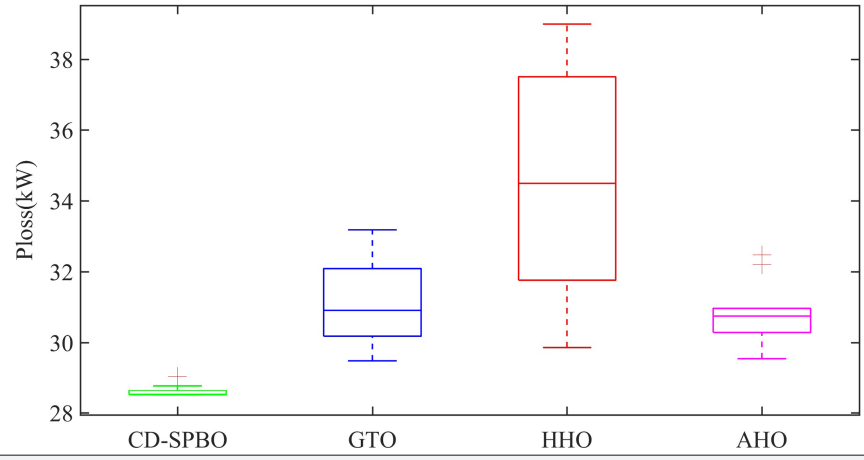

Fig. 10. Box plot for optimal allocation of two DGs and two D-STATCOMs in a 33-bus system. AHO, artificial hummingbird optimizer; CD-SPBO, continuous–discrete student psychology-based optimization; GTO, gorilla troop optimizer; HHO, Harris hawk optimizer.

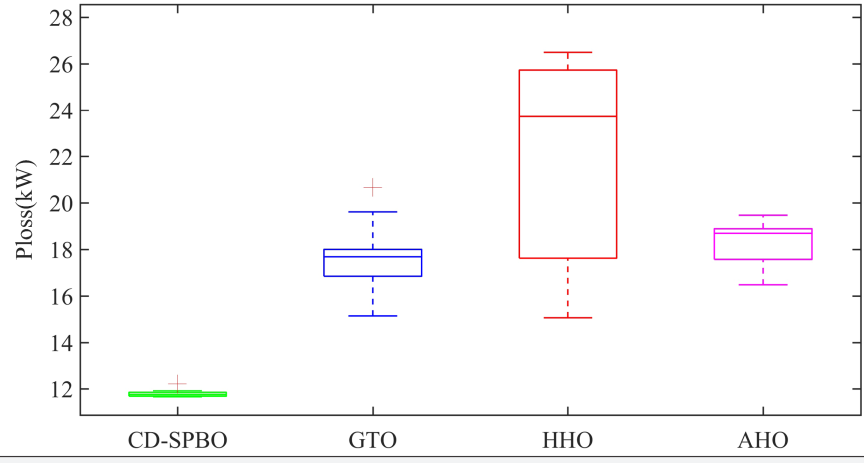

Fig. 11. Box plot for optimal allocation of three DGs and three D-STATCOMs in a 33-bus system. AHO, artificial hummingbird optimizer; CD-SPBO, continuous–discrete student psychology-based optimization; GTO, gorilla troop optimizer; HHO, Harris hawk optimizer.

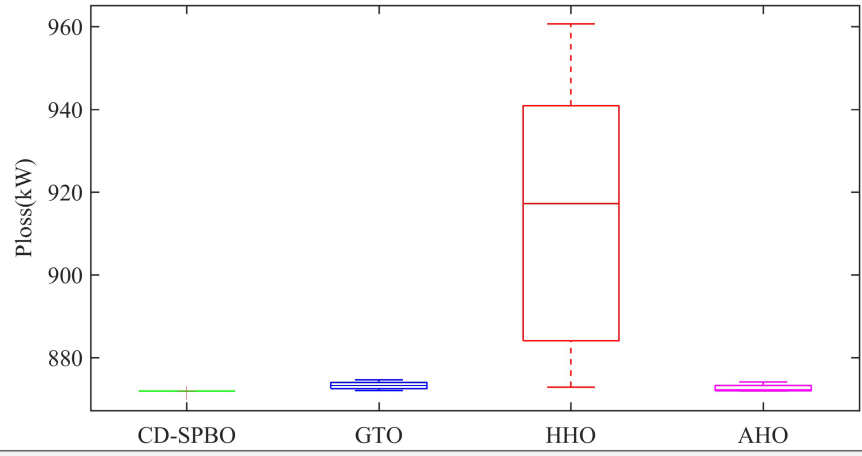

Fig. 12. Box plot for optimal allocation of one DG and one D-STATCOM in a 118-bus system. AHO, artificial hummingbird optimizer; CD-SPBO, continuous–discrete student psychology-based optimization; GTO, gorilla troop optimizer; HHO, Harris hawk optimizer.

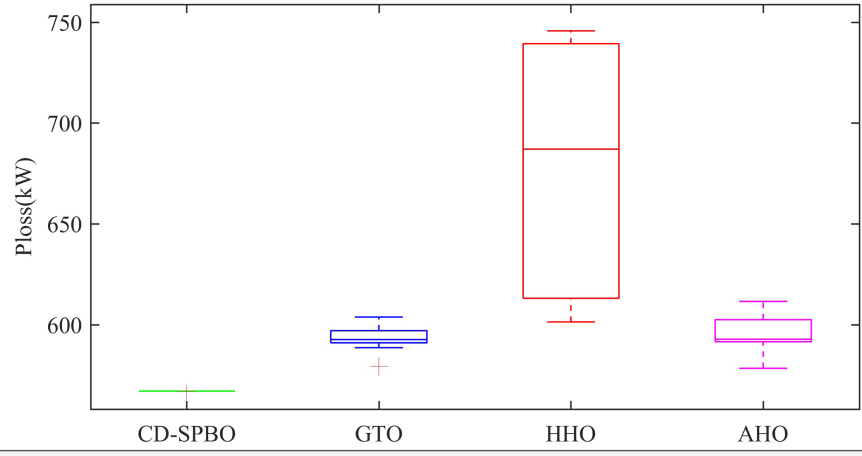

Fig. 13. Box plot for optimal allocation of two DGs and two D-STATCOMs in a 118-bus system. AHO, artificial hummingbird optimizer; CD-SPBO, continuous–discrete student psychology-based optimization; GTO, gorilla troop optimizer; HHO, Harris hawk optimizer.

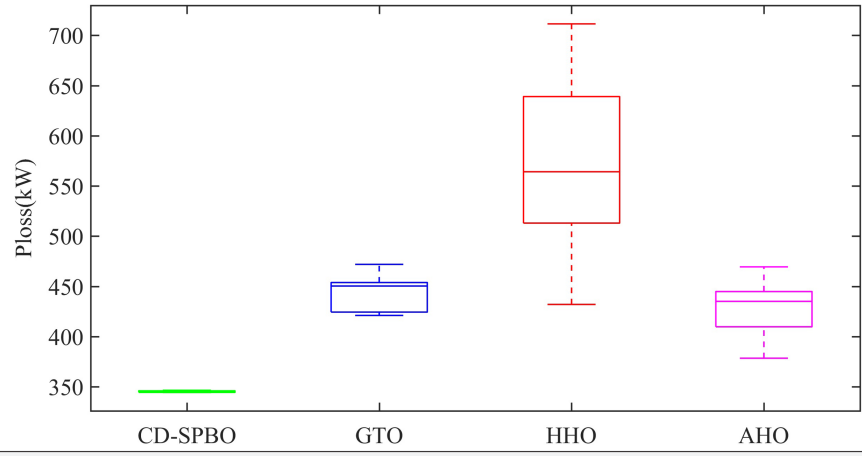

Fig. 14. Box plot for optimal allocation of three DGs and three D-STATCOMs in a 118-bus system. AHO, artificial hummingbird optimizer; CD-SPBO, continuous–discrete student psychology-based optimization; GTO, gorilla troop optimizer; HHO, Harris hawk optimizer.

TABLE V. PERFORMANCE COMPARISON OF 33-BUS APDN FOR DIFFERENT PLANNING SCENARIOS

Items	PS-I	PS-II	PS -III	PS -IV	PS -V	PS -VI	PS -VII
P_{DG}, kW	-	1.3114	1.0915	1.1474	1.0814	1.2583	1.2310
		1.3384	1.3138	0.9677	0.8108	0.9603	1.0075
		0.9363	0.8425	0.8326	1.0657	0.8065	0.8148
L_{DG}	-	24	24	24	30	24	24
		30	30	30	13	30	30
		13	13	13	24	13	13
Q_{DSTAT}, kVAr	0.8167	-	-	0.4219	0.1221	0.3886	0.3544
	0.9799			0.4862	0.4485	0.8920	0.3790
	0.5465			1.0000	0.2837	0.3569	0.3690
L_{DSTAT}	7	-	-	25	21	7	31
	30			12	7	30	25
	15			30	32	25	7
P_{loss}, kW	146.5795	78.6331	18.9542	12.3286	**11.2484**	11.8232	11.4939
V_{min} p.u..	0.9496	0.9803	0.9941	0.9940	**0.9956**	0.9941	0.9941
MOF, p.u.	0.6201	0.2735	0.1350	**0.0656**	0.1050	0.0734	0.0892

LDG, DG connected bus; LDSTAT, D-STATCOM connected bus; MOF, multi-objective function; P_{DG}, Real power injected by DG; P_{loss}, real power loss; PS, planning scenario; Q_{DSTAT}, reactive power injected by D-STATCOM; V_{min}, minimum bus voltage. Bold values represent the best values.

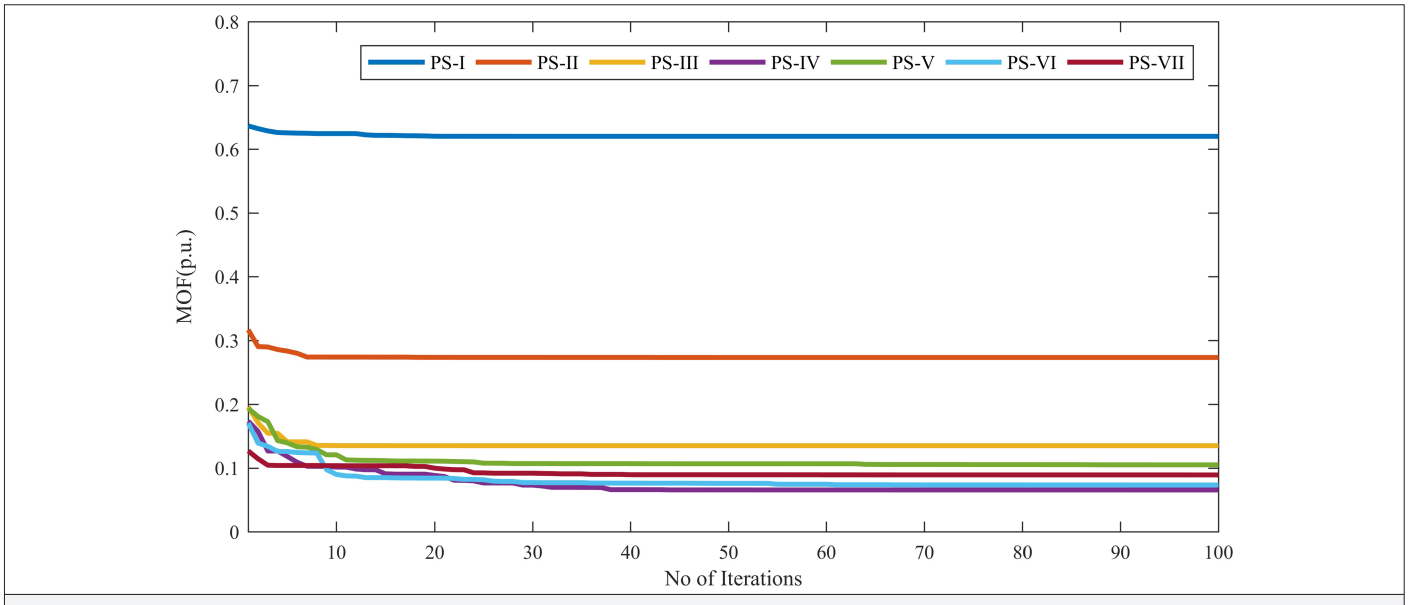

Fig. 15. Comparison of the convergence characteristics of CD-SPBO for the 33-bus system for different planning scenarios. PS, planning scenario.

Similarly, the variation of the VSI of the 33-bus APDN for all planning scenarios is shown in Fig. 17. This figure also suggests that the 33-bus APDN is more immune to voltage collapse for planning scenarios PS-III to PS-VII, as indicated by VSI values closer to unity.

In order to select the best planning scenario for 33-bus APDN, a comparison of techno-economic indices defined in the earlier sections, namely f_{APL}, f_{OVD}, f_{CVSI}, and f_{SAC} are compared in Fig. 18. It may be noted that the higher the value of these indices, the lesser are their impact on the performance enhancement of the APDN. Considering the value of f_{APL} as obtained for different scenarios, it is obvious that PS-I has the least impact on APL reduction, followed by PS-II. However, for planning scenarios PS-IV to PS-VII, f_{APL} values are closer to 0.05 indicating APL reduction of more than 95%. In terms of f_{OVD}, PS-I

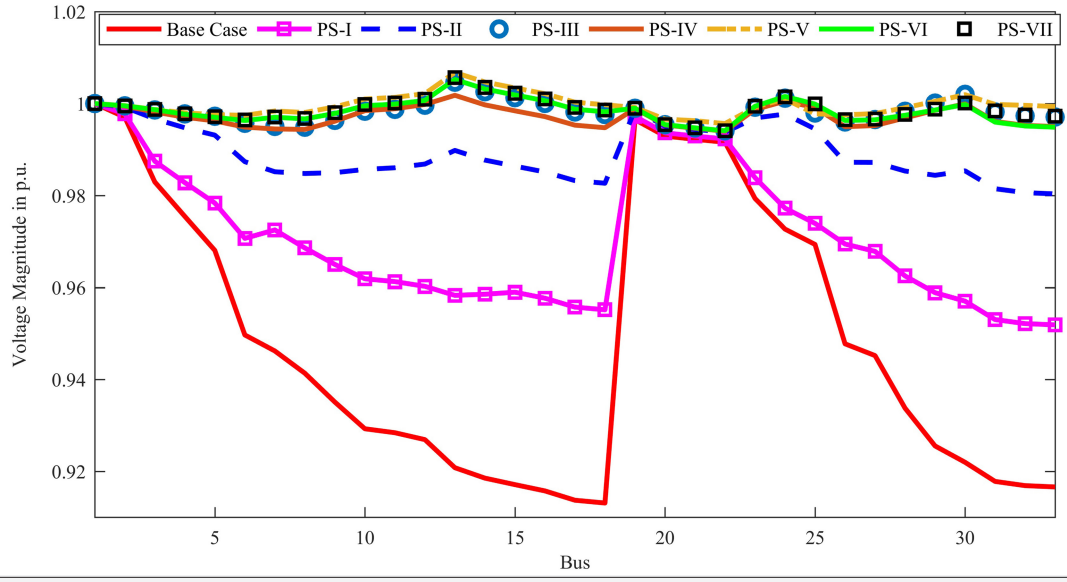

Fig. 16. Comparison of voltage profile of 33-bus system for different planning scenarios. PS, planning scenario.

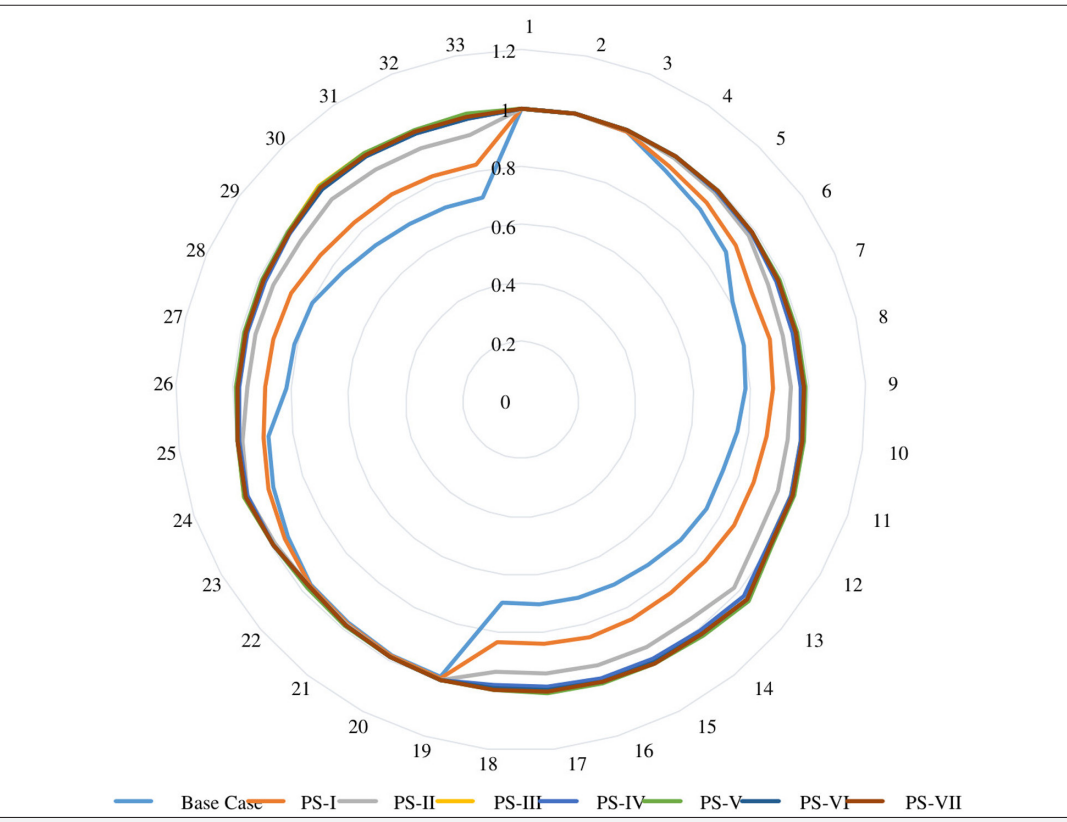

Fig. 17. Comparison of voltage stability index of the 33-bus system for different planning scenarios. PS, planning scenario.

has the least impact, followed by PS-II, and for the remaining scenarios, diminishingly small f_{OVD} indicates an almost flat voltage profile. Further, observing the variation of f_{CVSI}, once again, PS-I and PS-II can be readily discarded, whereas the remaining planning scenarios are inseparable with PS-V being marginally better in that lot. In contrast to the technical factors, the graph of f_{SAC} reveals some interesting facts, which along with the technical factors, can be decisive in selecting the best planning scenario. It is obvious from the plot that PS-I, which impacts the least in terms of technical factors, appears to be the best in terms of f_{SAC}. In contrast, PS-V, which has adjudged the best planning scenario in terms of technical factors, has performed the worst in terms of f_{SAC} because of incurring additional penalty cost for pollution caused by BM-DGs. Hence, both PS-I and PS-V are not suitable for concurrently optimizing the techno-economic

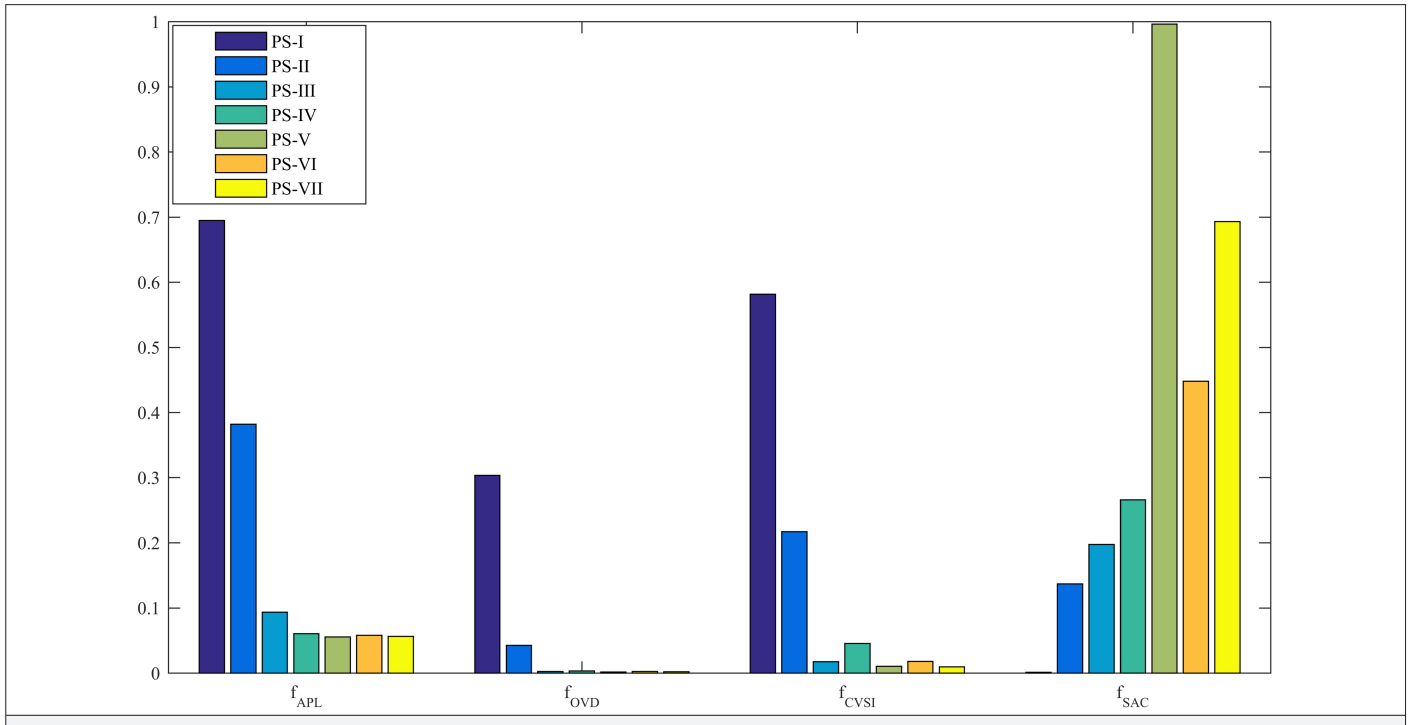

Fig. 18. Comparison of performance indices of 33-bus system for different planning scenarios. APL, active power loss; CVSI, critical voltage stability index; OVD, overall voltage deviation; PS, planning scenario; SAC, system annual cost.

TABLE VI. PERFORMANCE COMPARISON OF 118-BUS APDN FOR DIFFERENT PLANNING SCENARIOS

Items	PS-I	PS-II	PS -III	PS -IV	PS -V	PS -VI	PS -VII
P_{DG}, kW	-	3.8704	3.5252	1.1474	1.0814	1.2583	1.2310
		3.4615	3.2370	0.9677	0.8108	0.9603	1.0075
		3.0589	3.0190	0.8326	1.0657	0.8065	0.8148
L_{DG}	-	49	50	24	30	24	24
		71	71	30	13	30	30
		110	110	13	24	13	13
Q_{DSTAT}, kVAr	2.7412	-	-	0.4219	0.1221	0.3886	0.3544
	3.0000			0.4862	0.4485	0.8920	0.3790
	3.0000			1.0000	0.2837	0.3569	0.3690
L_{DSTAT}	110	-	-	25	21	7	31
	71			12	7	30	25
	50			30	32	25	7
P_{loss}, kW	936.3917	686.0218	384.4106	12.3286	**11.2484**	11.8232	11.4939
V_{min} p.u.	0.9178	0.9561	0.9603	0.9940	**0.9956**	0.9941	0.9941
MOF, p.u.	0.6825	0.4652	0.3634	**0.0656**	0.1050	0.0734	0.0892

LDG, DG connected bus; LDSTAT, D-STATCOM connected bus; MOF, multi-objective function; P_{DG}, real power injected by DG; P_{loss}, real power loss; PS, planning scenario; Q_{DSTAT}, reactive power injected by D-STATCOM; V_{min}, minimum bus voltage. Bold values represent the best values

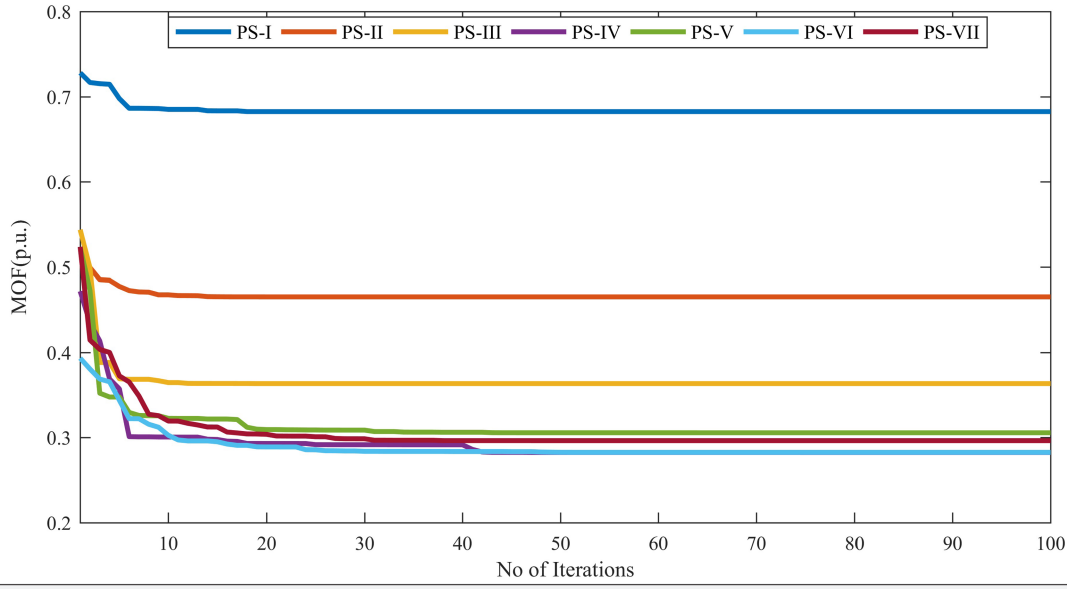

Fig. 19. Comparison of the convergence characteristics of CD-SPBO for the 118-bus system for different planning scenarios. PS, planning scenario.

performance of the APDN. However, considering both technical and economic feasibility, PS-VI, IV, and PS-VII are more favorable for the DUs, with PS-IV being comparatively more economical and PS-VII being comparatively more technically promising.

2) 118-bus APDN

The results obtained by CD-SPBOA for minimizing the proposed MOF considering different planning scenarios for a 118-bus APDN are presented in Table VI. From Table VI, it may be noted that the reduction in APL and improvement in voltage profile is better and more or less similar for planning scenarios involving simultaneous allocation of both DGs and D-STATCOMs (PS-IV to PS-VII) owing to the concurrent real and reactive power injection compared to exclusive device allocation. Furthermore, in PS-V, additional reactive power is also supported by BM-DGs in addition to that of D-STATCOMs, leading to maximum APL reduction and enhanced voltage profile compared to the remaining scenarios. However, in terms of overall performance improvement, PS-IV has delivered the best, followed by PS-VI, as indicated by the least MOF values reported in Table VI.

The convergence characteristics of CD-SPBOA for minimizing the proposed MOF considering different planning scenarios for 118-bus are depicted in Fig. 19. It shows that CD-SPBOA converges swiftly to the optimal value for all planning scenarios and attains the minimum

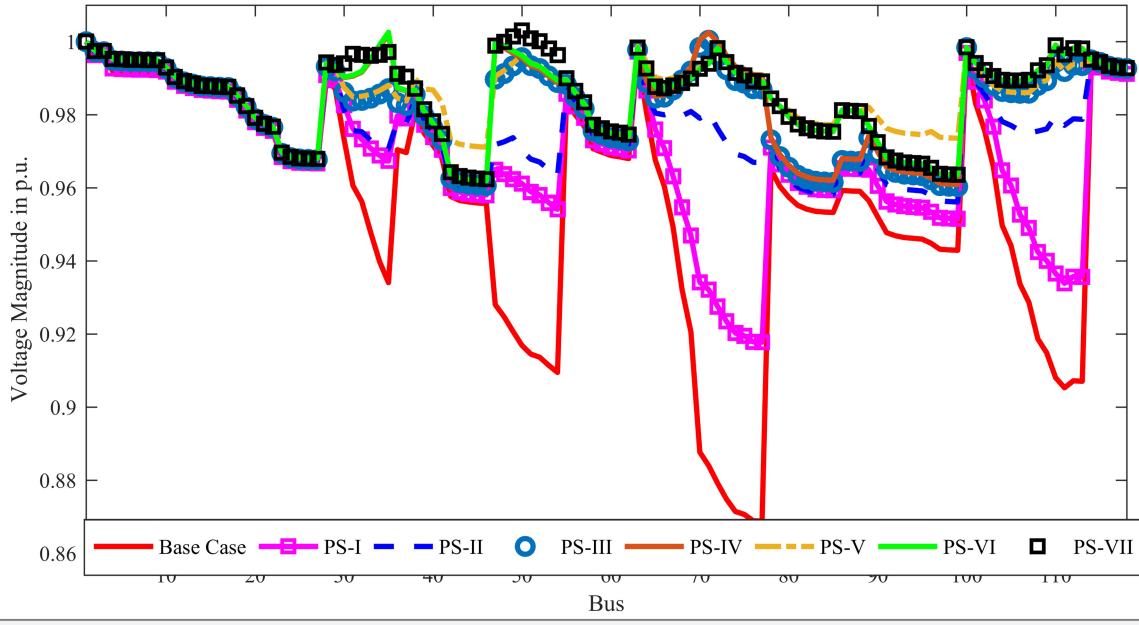

Fig. 20. Comparison of voltage profile of 118-bus system for different planning scenarios. PS, planning scenario.

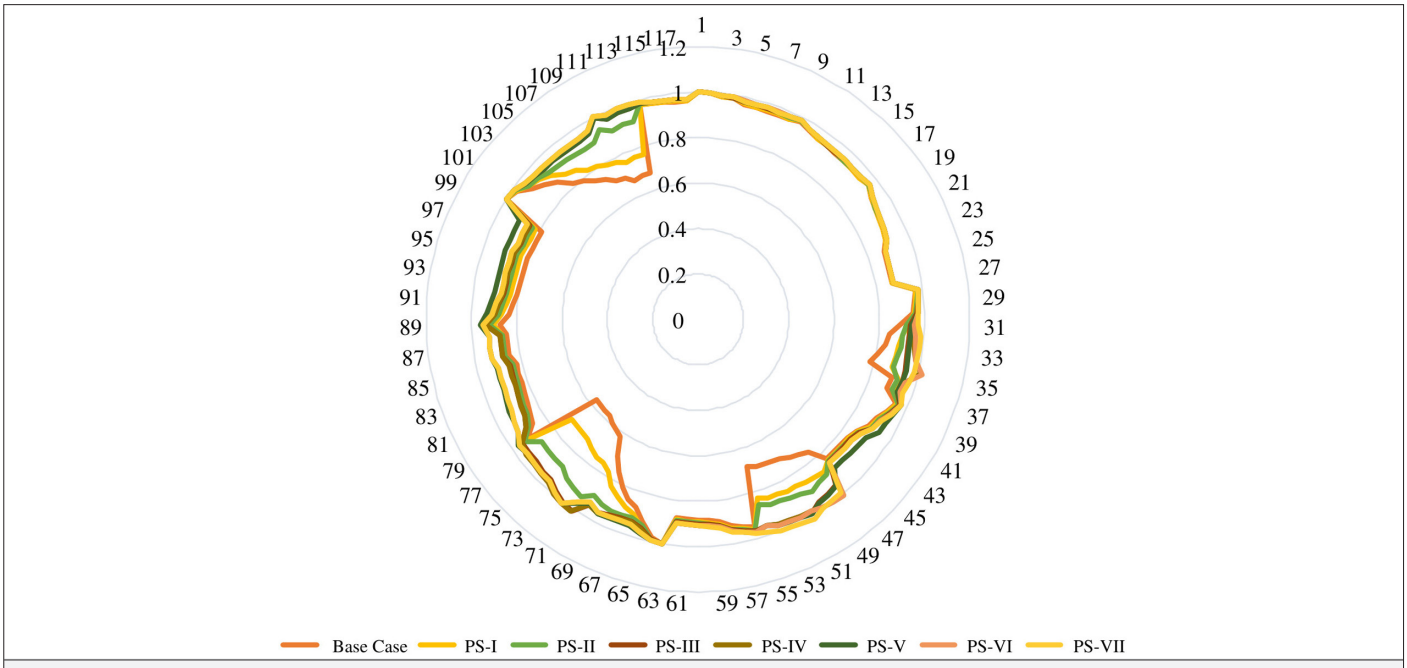

Fig. 21. Comparison of voltage stability index of the 118-bus system for different planning scenarios. PS, planning scenario.

MOF for PS-IV followed by PS-VI. The voltage profile of 118-bus APDN corresponding to all planning scenarios is also compared in Fig. 20. It displays that the base case voltage profile of 118-bus APDN is not acceptable as many of the bus's voltage magnitudes are less than the regulatory limits of 0.95 p.u. However, for planning scenarios PS-III to PS-VII, the voltage profile of the network is significantly improved. Similarly, the variation of the VSI of the 118-bus APDN for all planning scenarios is shown in Fig. 21. This figure also suggests that the 118-bus APDN is more immune to voltage collapse for planning scenarios PS-III to PS-VII, as indicated by VSI values closer to unity.

A comparison of techno-economic indices defined in the earlier sections, namely f_{APL}, f_{OVD}, f_{CVSI}, and f_{SAC} are compared in Fig. 22 for 118-bus

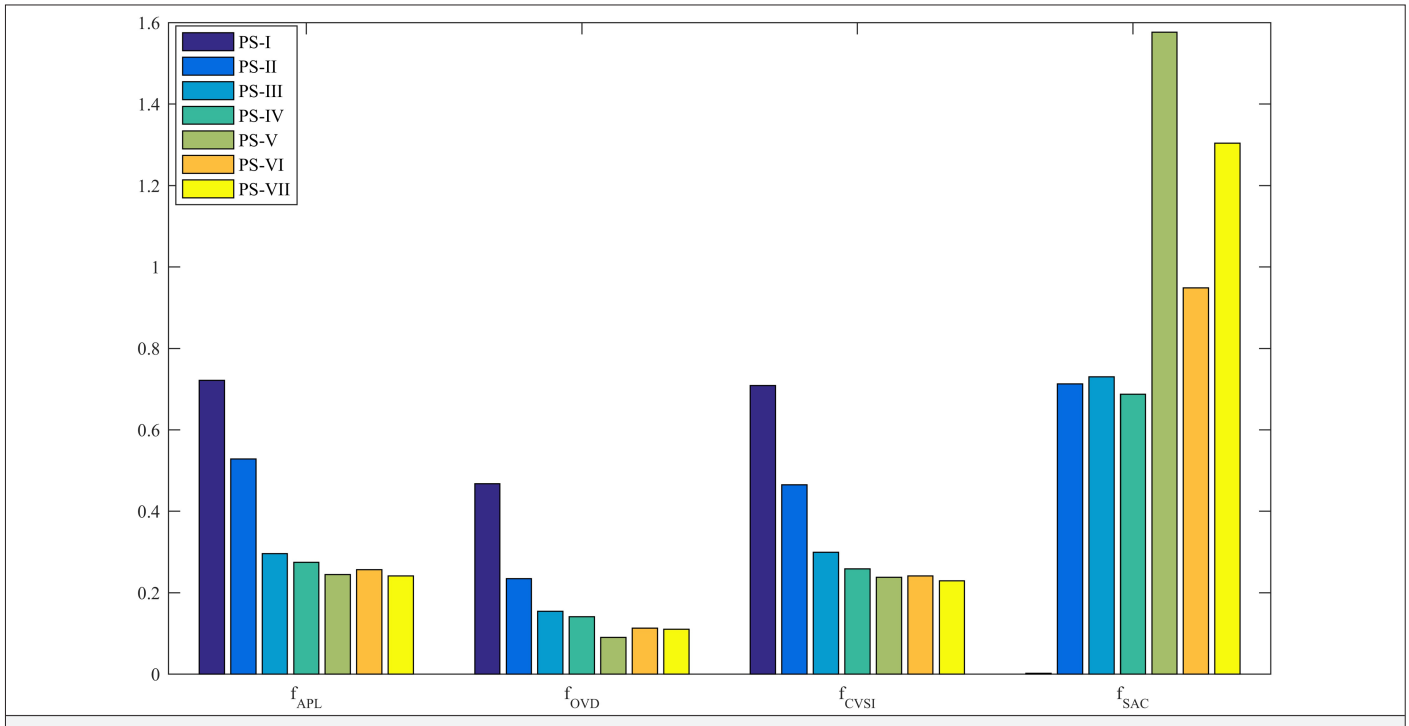

Fig. 22. Comparison of performance indices of the 118-bus system for different planning scenarios. APL, active power loss; CVSI, critical voltage stability index; OVD, overall voltage deviation; PS, planning scenario; SAC, system annual cost.

TABLE VII. VARIATION OF V_{MIN} AND P_{LOSS} WITH LOAD FACTOR OF THE 33-BUS SYSTEM

	Base Case		PS-IV		PS-VI		PS-VII	
Load Factor	**V_{min} p.u.**	**P_{loss} kW**	**V_{min} p.u.**	**Ploss kW**	**V_{min} p.u.**	**Ploss kW**	**V_{min} p.u.**	**P_{loss} kW**
0.5	0.9540	48.7853	0.9836	9.8094	0.9825	9.5689	0.9813	10.2280
0.6	0.9443	71.3029	0.9836	10.5414	0.9830	10.1078	0.9819	10.5911
0.7	0.9345	98.5338	0.9847	10.5856	0.9848	9.9592	0.9840	10.1533
0.8	0.9244	130.7165	0.9870	10.3803	0.9879	9.6236	0.9875	9.4996
0.9	0.9142	168.1063	0.9903	10.6295	0.9909	9.8843	0.9920	9.5365
1.0	0.9038	210.9824	0.9940	12.2821	0.9941	11.7827	0.9941	11.4619
1.1	0.8931	259.6507	0.9917	15.0459	0.9919	14.3642	0.9935	13.9469
1.2	0.8822	314.4989	0.9883	19.2834	0.9889	18.0271	0.9928	16.9604

P_{loss}, real power loss; PS, planning scenario; V_{min}, minimum bus voltage.

APDN. Considering the value of f_{APL} as obtained for different scenarios, it is obvious that PS-I and PS-II are not promising to curb APL, as for both scenarios, f_{APL} is more than 0.5. For the remaining scenarios, f_{APL} ranges within 0.3 to 0.2, indicating a loss reduction of (70 to 80) % compared to the base case.

In terms of f_{OVD}, PS-I has the least impact, followed by PS-II, and for the remaining scenarios except PS-V, f_{OVD} values are slightly higher than 0.1, whereas for PS-V it is lesser than 0.1, ensuring a more flat voltage profile. Further, observing the variation of f_{CVSI}, once again, PS-I and PS-II can be readily discarded, whereas the remaining planning scenarios are in close agreement with PS-V being marginally better in that lot. In contrast to the technical factors, the graph of f_{SAC} reveals some interesting facts, which along with the technical factors, can be decisive in selecting the best planning scenario. It is obvious from the plot that PS-I, which impacts the least in terms of technical factors, appears to be the best in terms of f_{SAC}. In contrast, the planning scenarios PS-V and PS-VII are economically infeasible as their f_{SAC} values are greater than unity. However, considering both technical and economic feasibility, PS-IV may be considered as the optimal planning scenario for 118-bus APDN.

D. Effect of Load Variation on Performance of APDN for OADD

In this section, the effect of load variation on optimal planning scenarios is discussed. Therefore, the loads across all feeders were uniformly increased from 50% of nominal loading to 120% of the nominal loading in steps of 10%. As it is established in an earlier section, planning scenarios PS-IV, PS-VI, and PS-VII are more favorable for overall performance enhancement of the 33-bus APDN. Table VII compares the variation of V_{min} and power loss with respect to variation in load factor for the said planning scenarios, including base case. As evident from the table, the APL reduction for loading scenarios is significantly better for PS-IV, PS-VI, and PS-VII as compared to the base case. Additionally, the voltage profile is well within the regulatory limits for PS-IV, PS-VI, and PS-VII as compared to the base case.

VI. CONCLUSION

In this paper, optimum planning techniques for active DNs in the presence of solar PV DGs, BM DGs, and D-STATCOMs have been carried out. The proposed CD-SPBO algorithm has been validated by considering the simultaneous allocation of one, two, and three pairs of DGs and D-STATCOMs for minimizing real power loss of a 33-bus and a bigger 118-bus test system comparing its results with both state-of-the-art methods as well as recently surfaced metaheuristic approaches such as GTO, AHO, and HHO, the comparison reveals that numerical and statistical performance (convergence speed, robustness through box plots, and avoidance of local optima) of the proposed CD-SPBO is superior for optimal planning of the DN.

Further, a novel MOF has been developed to account for technological, economic, and environmental benefits. The weights of the various indices utilized in the MOF, such as f_{APL}, f_{OVD}, f_{CVSI}, and f_{SAC}, have been generated from AHP in order to restrict their influence on the final optimization outcomes using the proposed CD-SPBO algorithm. The best allocation techniques for DGs and D-STATCOMs have been determined using the proposed CD-SPBO algorithm. Seven separate scenarios have been used to demonstrate the usefulness of the suggested solution approach for 33-bus and 118-bus APDN. The results reveal that the exclusive allocation of D-STATCOMs, PV-DGs, and BM-DGs has a reduced effect on both technical and economic performance of the studied test systems compared to concurrent optimal allocation of devices. It has been observed that considerable improvements in technical performance, as well as economic and environmental issues, occur when two PV-DGs, one BM-DG, and three D-STATCOMs are allocated concurrently. Additionally, the results indicate that when two PV-DGs, one BM-DG, and three D-STATCOMs are appropriately placed, the influence of incremental load changes is minimized for the considered APDNs. So, it can be concluded that the proposed methodology can be beneficial for network planners in determining the best combination of devices to meet their needs. This work can further be extended for stochastic DN planning considering generation and load uncertainties.

Peer-review: Externally peer-reviewed.

Author Contributions: Concept – S.K.D., S.M.; Design – S.K.D., S.M.; Supervision – S.M.; Materials – S.K.D.; Data Collection and/or Processing – S.K.D.; Analysis and/or Interpretation – S.K.D., S.M.; Literature Review – S.K.D., S.M.; Writing – S.K.D., S.M.; Critical Review – S.K.D., S.M.

Declaration of Interests: The authors declare that they have no competing interests.

Funding: The authors declared that this study has received no financial support.

REFERENCES

1. A. Kumar, R. Verma, N. K. Choudhary, and N. Singh, "Optimal placement and sizing of distributed generation in power distribution system: A comprehensive review," *Energy Sources A*, vol. 45, no. 3, pp. 7160–7185, 2023. [CrossRef]
2. T. S. L. V. Ayyarao, and P. P. Kumar, "Parameter estimation of solar PV models with a new proposed war strategy optimization algorithm," *Int. J. Energy Res.*, vol. 46, no. 6, pp. 7215–7238, 2022. [CrossRef]
3. S. Barik, and D. Das, "A novel Q – PQV bus pair method of biomass DGs placement in distribution networks to maintain the voltage of remotely located buses," *Energy*, vol. 194, no. 1, 2020. [CrossRef]
4. S. K. Dash, S. Mishra, and A. Y. Abdelaziz, "A critical analysis of modeling aspects of D-STATCOMs for optimal reactive power compensation in power distribution networks," *Energies*, vol. 15, no. 19, p. 6908, 2022. [CrossRef]
5. R. Sirjani, and A. Rezaee Jordehi, "Optimal placement and sizing of distribution static compensator (D-STATCOM) in electric distribution networks: A review." *Renew. Sustain. Energy Rev.*, vol. 77, pp. 688–694, 2017. [CrossRef]
6. A. A. A. El-Ela, S. M. Allam, A. M. Shaheen, and N. A. Nagem, "Optimal allocation of biomass distributed generation in distribution systems using equilibrium algorithm," *Int. Trans. Electr. Energy Syst.*, vol. 31, no. 2, 2021.
7. A. A. Fathy, "A novel artificial hummingbird algorithm for integrating renewable based biomass distributed generators in radial distribution systems," *Appl. Energy*, vol. 323, 2022. [CrossRef]
8. A. F. A. Kadir, T. Khatib, L. S. Lii, and E. E. Hassan, " Optimal placement and sizing of photovoltaic based distributed generation considering costs of operation planning of monocrystalline and thin-film technologies," *J. Sol. Energy Eng.*, vol. 141, no.1, 2019.
9. S. K. Dash, and S.Mishra, "Optimal allocation of photo-voltaic units in radial distribution networks using a new student psychology based optimization algorithm," *Int. J. Electr. Eng. Inform.*, vol. 13, no.2, 318–335, 2021. [CrossRef]
10. M. A. Hamidan, and F. Borousan, "Optimal planning of distributed generation and battery energy storage systems simultaneously in distribution networks for loss reduction and reliability improvement," *J. Energy Storage*, vol. 46, p. 103844, 2022. [CrossRef]
11. B. Khan, K. Redae, E. Gidey, O. P. Mahela, I. B. M. Taha, and M. G. Hussien, "Optimal integration of DSTATCOM using improved bacterial search algorithm for distribution network optimization," *Alex. Eng. J.*, vol. 61, no. 7, pp. 5539–5555, 2022. [CrossRef]
12. S. Ganesh, and R. Kanimozhi, "Meta-heuristic technique for network reconfiguration in distribution system with photovoltaic and D-STATCOM," *IET Gener. Transm. Distrib.*, vol.12, no. 20, pp. 4524–4535, 2018. [CrossRef]
13. T. Yuvaraj, and K. Ravi, "Multi-objective simultaneous DG and DSTATCOM allocation in radial distribution networks using cuckoo searching algorithm," *Alex. Eng. J.*, vol. 57, no. 4, pp. 2729–2742, 2018. [CrossRef]
14. T.Yuvraj, K. R. Devabalaji, "Simultaneous allocation of DG and DSTATCOM using whale optimization algorithm," *Iran. J. Sci. Technol. Trans. Electr. Eng.*, vol. 44, no. 2, pp. 879–896, 2020. [CrossRef]
15. S. G. R. Chinnaraj, and R. Kuppan, "Optimal sizing and placement of multiple renewable distribution generation and DSTATCOM in radial distribution systems using hybrid lightning search algorithm-simplex method optimization algorithm," *Comput. Intell.*, vol.37, no. 4, pp. 1673–1690, 2021. [CrossRef]
16. M. H. Ali, S. Kamel, M. H. Hassan, M. Tostado-Véliz, and H. M. Zawbaa, "An improved wild horse optimization algorithm for reliability based optimal DG planning of radial distribution networks," *Energy Rep.*, vol. 8, pp. 582–604, 2022. [CrossRef]
17. R. Sellami, F. Sher, and R. Neji, "An improved MOPSO algorithm for optimal sizing & placement of distributed generation: A case study of the Tunisian offshore distribution network (ASHTART)," *Energy Rep.*, vol. 8, pp. 6960–6975, 2022. [CrossRef]
18. M. A. Tolba, E. H. Houssein, A. A. Eisa, and F. A. Hashim, "Optimizing the distributed generators integration in electrical distribution networks: Efficient modified forensic-based investigation," *Neural Comput. Appl.*, vol. 35, no. 11, pp. 8307–8342, 2023. [CrossRef]
19. R. Fathi, B. Tousi, and S. Galvani, "Allocation of renewable resources with radial distribution network reconfiguration using improved salp swarm algorithm," *Appl. Soft Comput.*, vol. 132, 2023. [CrossRef]
20. O. D. Montoya, A. Molina-Cabrera, D. A. Giral-Ramírez, E. Rivas-Trujillo, and J. A. Alarcón-Villamil, "Optimal integration of D-STATCOM in distribution grids for annual operating costs reduction via the discrete version sine-cosine algorithm," *Results Eng.*, vol. 16, 2022. [CrossRef]
21. W. Gil-González, "Optimal placement and sizing of D-STATCOMs in electrical distribution networks using a stochastic mixed-integer convex model," *Electronics*, vol. 12, no. 7, 2023. [CrossRef]
22. M. A. Elseify, F. A. Hashim, A. G. Hussien, and S. Kamel, "Single and multi-objectives based on an improved golden jackal optimization algorithm for simultaneous integration of multiple capacitors and multi-type DGs in distribution systems," *Appl. Energy*, vol. 353, 2024. [CrossRef]
23. M. A. Elseify, S. Kamel, L. Nasrat, and F. Jurado, "Multi-objective optimal allocation of multiple capacitors and distributed generators considering different load models using Lichtenberg and thermal exchange optimization techniques," *Neural Comput. Appl.*, vol. 35, no. 16, pp.11867–11899, 2023. [CrossRef]
24. J. Qian, P. Wang, C. Pu, X. Peng, and G. Chen, "Application of effective gravitational search algorithm with constraint priority and expert experience in optimal allocation problems of distribution network," *Eng. Appl. Artif. Intell.*, vol. 117, 2023. [CrossRef]
25. A. F. Raj, and A. G. Saravanan, "An optimization approach for optimal location & size of DSTATCOM and DG," *Appl. Energy*, vol. 336, 2023.
26. B. Das, V. Mukherjee, and D. Das, "Student psychology-based optimization algorithm: A new population-*based* optimization algorithm for solving optimization problems," *Adv. Eng. Softw.*, vol. 146, 2020. [CrossRef]
27. K. Balu, and V. Mukherjee, "Optimal siting and sizing of distributed generation in radial distribution system using a novel student psychology-based optimization algorithm," *Neural Comput. Appl.*, vol. 33, no. 22, pp.15639–15667, 2021. [CrossRef]
28. A. Eid, S. Kamel, H. M. Zawbaa, and M. Dardeer, "Improvement of active distribution systems with high penetration capacities of shunt reactive compensators and distributed generators using Bald Eagle Search," *Ain Shams Eng. J.*, vol. 13, no. 6, 2022. [CrossRef]
29. K. Babu, and S. Maheswarapu, "New hybrid multiverse optimisation approach for optimal accommodation of DGs in power distribution networks," *IET Gener. Transm. Distrib.*, vol. 13, no. 13, pp. 2673–2685, 2019. [CrossRef]
30. S. Mishra, D. Das, and S. Paul, "A comprehensive review on power distribution network reconfiguration," *Energy Syst.*, vol. 8, no. 2, pp.227–284, 2017. [CrossRef]
31. S. Mishra, "A simple algorithm for unbalanced radial distribution system load flow," in Proc. TENCON 2008 IEEE Region 10 Conf., Hyderabad, India, 19–21 November 2019, pp. 1–6, 2008. [CrossRef]
32. F. Iqbal, M. T. Khan, and A. S. Siddiqui, "Optimal placement of DG and DSTATCOM for loss reduction and voltage profile improvement," *Alex. Eng. J.*, vol. 57, no. 2, pp. 755–765, 2018. [CrossRef]
33. K. Ibrahim, R. Sirjani, and H. Shareef, "Performance assessment of Pareto and non-Pareto approaches for the optimal allocation of DG and DSTATCOM in the distribution system," *Tech. Gaz.*, vol. 27, no. 5, pp. 1654–1661, 2020.

Dr. Sivkumar Mishra received the B. E degree from Malaviya Reginal Engineering College, Jaipur (presently known as Malaviya National Institute of Technology, Jaipur) in 1995, M. Tech (Power System Engineering) from Indian Institute of Technology, Kharagpur and PhD (Engineering) from Jadavpur University, Kolkata. He is currently working as Professor in Center for Under Graduate and Post Graduate Studies, Biju Patnayak University of Technology, Odisha, Rourkela. His research interests include Intelligent Methods for Power System Planning and Smart Grid related Studies. He is a Senior Member of IEEE and IEEE Power and Energy Society.

Dr. Subrat Kumar Dash is presently working as an Assistant Professor in the Department of Electrical Engineering, Government College of Engineering, Kalahandi, India. He graduated in Electrical and Electronics Engineering from Biju Patnayak University of Technology, Odisha, Rourkela in the year 2007. He received the M. Tech degree in Electrical Engineering from Indian Institute of Technology, Kharagpur in 2013 and PhD (Engineering) from Biju Patnayak University of Technology. His research interests include Electrical Distribution System Planning, Soft Computing Application to Power System and DFACTS devices. He is a Member of IEEE and IEEE Power and Energy Society.